age (Fig. 5C, 170% of age-matched male mice). However, no statistical difference was detected between genders at 16 and 23 months of age: 197% vs 219% and 209% vs 236% in male vs female mice, respectively. sAPPbeta levels were significantly increased with aging compared to mice at 9 months of age: 100%→197%→209% in male mice, 170%→219%→236% in female mice at 9, 16 and 23 months of age, respectively.

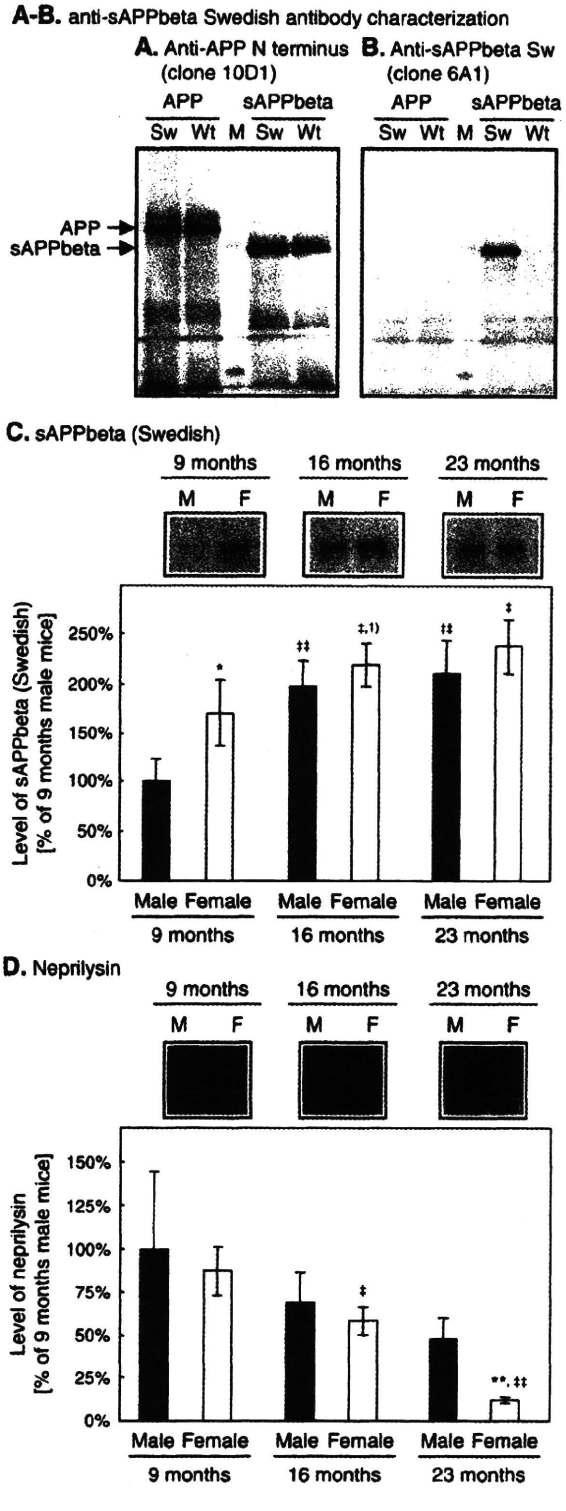

Neprilysin levels were not different between genders at 9 and 16 months of age; 100% vs 87%, 68% vs 58% in male and female mice at 9 and 16 months of age, respectively (Fig. 5D). At 23 months of age, neprilysin levels were significantly reduced in female mice compared to age-matched male mice (47% vs 12%, respectively). Compared to gender-matched 9 month old mice, female mice showed greater reduction with aging than males; 100%→68%→47% in male mice, 87%→58%→12% in female mice at 9, 16 and 23 months of age, respectively.

2.6. *Tau pathology was not influenced by gender*

To determine whether gender difference affected tau phosphorylation as it did Abeta, we examined levels of phosphorylated tau in male and female mice at 9, 16 and 23 months of age. Levels of phosphorylated tau were markedly increased with aging (Matsuoka et al., unpublished observation). Levels of phosphorylated tau in female mice at a given age were compared with age-matched male mice. No statistically significant gender difference was detected at any of these ages (Fig. 6).

3. Discussion

Epidemiological studies indicate that women have a higher risk of AD even after adjustment for age (Brookmeyer et al., 1998), the most important risk factor for AD (Hy and Keller, 2000). Transgenic mice expressing pathogenic genes of AD develop Abeta and/or tau pathology (McGowan et al., 2006); however, previous studies of AD transgenic mouse models have not necessarily reflected a consistent gender difference. In Tg2576 mice, the Abeta 1–40 level has been reported to be higher in females than males (~115% in soluble Abeta 1–40 and ~180% in total Abeta 1–40 in females compared to males), but

Fig. 5 – Female mice have higher beta-secretase activity and lower neprilysin levels. Antibodies specific to APP N-terminus and Swedish-type sAPPbeta, clones 10D1 and 6A1, were characterized (A and B, respectively). Levels of sAPPbeta (C) and neprilysin (D) were compared and densitometrically quantified between genders at 9, 16 and 23 months of age. A–B: COS1 cells transfected with wild-type- (Wt) or Swedish mutant (Sw) type-full-length APP or sAPPbeta were run on a gel and probed with antibodies against APP N-terminus and Swedish sAPPbeta, clones 10D1 and 6A1, respectively. C: sAPPbeta level was significantly higher in female compared to male 3xTg-AD mice at 9 months of age. However, there is no significant difference between genders at older ages, 16 and 23 months of age. sAPPbeta levels were significantly elevated at 16 and 23 months of age compared to gender-matched mice at 9 months of age. D: Neprilysin levels decrease with advancing age in both male and female 3xTg-AD mice, with the magnitude of the decrease being greater in female mice. [1)]P=0.062, *P<0.05, **P<0.01 compared with age-matched male mice using t-test. ‡P<0.05, ‡‡P<0.01 compared with gender-matched mice at 9 months of age using ANOVA.

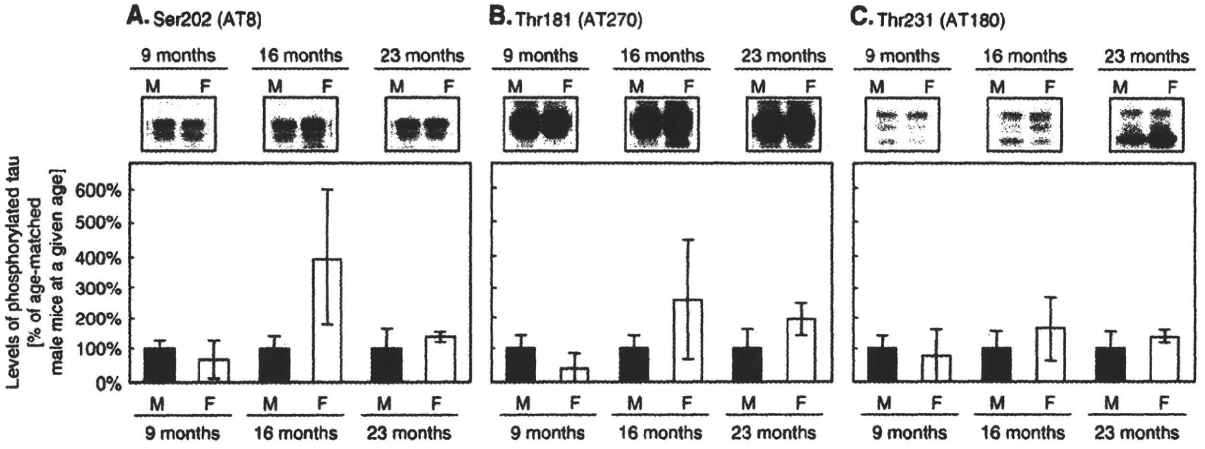

Fig. 6 – Gender difference had no effect on tau phosphorylation status. Levels of phosphorylated tau in unfractionated total tau were compared between age-matched female and male mice at 9, 16 and 23 months of age; i.e. 100% at each age point represents the level of phosphorylated tau in male mice at a given age. Since levels of phosphorylated tau were drastically increased with aging, the immunoblots from 9 and 23 months of age were outside the linear dynamic range in a single gel of immunoblotting. We therefore compared male and female mice brain homogenate side-by-side at a given age to examine gender differences. No statistically significant difference was detected.

levels of Abeta 1–42 were not different at 15 months of age (Abeta levels were not determined by ELISA at other ages) (Callahan et al., 2001). In our study, we compared Abeta levels at pre- and post-plaque pathological stages, and found that the gender difference in Abeta level became significant only after Abeta plaques were formed. Interestingly, the magnitude of the gender difference was much more significant in 3xTg-AD mice (161–648% depending on Abeta species and ages of mice) compared to Tg2576 mice. We also found that Abeta production and metabolism also affected by gender difference in 3xTg-AD mice. These findings suggest that 3xTg-AD mice may be useful as tools to investigate causes of gender differences in AD.

This study suggests possible causes of the higher risk of AD in women. The Abeta degrading enzyme neprilysin (Iwata et al., 2005) was significantly reduced with aging as previously reported in wild-type (non-transgenic) mice (Iwata et al., 2002) and AD mouse models (Caccamo et al., 2005; Lazarov et al., 2005). The decrease of neprilysin level found in 3xTg-AD mice was more exacerbated than that found in wild-type mice (Iwata et al., 2002), and notably, the reduction of neprilysin level was more prominent in female mice. Ovariectomy significantly reduces brain neprilysin activity and estrogen replacement restored the reduced neprilysin activity to the level in sham-operated mice (Huang et al., 2004), suggesting that expression or activity of neprilysin is in part regulated by estrogen in females, and supporting out finding. We found that Abeta level was not different between genders when mice were free from plaque pathology, though the sAPPbeta level, which reflects beta-secretase activity, was significantly higher in female mice. With aging, beta-secretase activity was increased as found in AD postmortem cases (Fukumoto et al., 2002; Holsinger et al., 2002; Yang et al., 2003; Zhao et al., 2007). These findings suggest that both up-regulation of Abeta production and down-regulation of Abeta degradation may contribute to the higher risk of AD in women.

Loss of ovarian steroids, particularly estrogens, at menopause may increase the susceptibility of the aging brain to AD neurodegeneration (Gandy and Duff, 2000), and estrogen is central to the current hypothesis on the gender difference in risk of AD. However, the effects of estrogen reduction through ovariectomy and hormone replacement therapy in transgenic models of AD are not completely consistent; ovariectomy increases the amount of Abeta and estrogen replacement therapy reduces Abeta in Tg2576 and PS/APP mice (Zheng et al., 2002), but not in PDAPP mice (Green et al., 2005). Although the majority of retrospective and prospective epidemiological studies suggest a beneficial effect of estrogen (Tang et al., 1996; Kawas et al., 1997; Waring et al., 1999; Zandi et al., 2002), clinical trials have shown conflicting results. In humans, three double-blind placebo-controlled clinical trials failed to detect beneficial effects of estrogen replacement therapy (Henderson et al., 2000; Mulnard et al., 2000; Wang et al., 2000). Estrogen has a variety of roles in addition to classic sex hormone function, including effects on neurotransmission (Mukai et al., 2006), which may complicate the overall outcomes in animal studies. Further studies investigating CNS estrogen-related signaling are required to elucidate the role of estrogen in AD pathology.

In the amyloid hypothesis, tau abnormalities are considered to be downstream of Abeta pathology (Hardy and Selkoe, 2002), and evidence supports this hypothesis. Abeta advances tau phosphorylation and neurofibrillary tangle formation in vivo (Lewis et al., 2001; Gotz et al., 2001), and reduction of endogenous tau ameliorates Abeta-induced effects in vivo (Roberson et al., 2007). However, it is not completely clear whether Abeta pathology is the major determinant of tau pathology and synaptic dysfunction. Abeta reduction ameliorated tau pathology at earlier, but not at later, pathological stages in 3xTg-AD mice (Oddo et al., 2004). Treatment with lithium chloride, a glycogen synthase kinase 3 inhibitor, reduced tau phosphorylation, but did not reduce Abeta load or improve cognitive performance in 3xTg-AD mice (Caccamo

et al., 2007). A neuronal tubulin-interacting peptide, NAPV-SIPQ, reduced tau phosphorylation and insoluble tau, and also improved cognitive impairment without reducing Abeta load in 3xTg-AD mice (Matsuoka et al., 2008). Taken together, although evidence supports the Abeta hypothesis overall, the relationship between Abeta and tau pathologies is not straightforward. While there are some reports suggesting that estrogen-related signaling may be also involved in tau phosphorylation in cultured cells in vitro (varez-de-la-Rosa et al., 2005), our in vivo study revealed that female mice show more aggressive Abeta pathology, although levels of phosphorylated tau were similar between genders. This suggests that the Abeta pathway, rather than the tau pathway, is dominantly involved in the higher risk of AD in women. Further studies are necessary to address the role of tau pathology in the higher risk of AD in women.

This transgenic mouse line was originally created by a group at the University of California, Irvine (Oddo et al., 2003). In the process of investigating gender differences, we also examined the progression of Abeta pathology at additional age points using strictly-defined groups with small age variance, specific gender and larger sample size. Although there are some discrepancies in the finding of intraneuronal Abeta, other key pathological features, such as Abeta plaques, hyperphosphorylated tau-bearing neurons, and thioflavin T-positive mature neurofibrillary tangles were found in 3xTg-AD mice housed at Georgetown University as originally reported (Oddo et al., 2003). However, the progression of pathology in our colony is slower than that reported in the original report (Oddo et al., 2003), and other investigators found similar slow progression of pathology at their institute (Drs. Donna M. Barten and Margi Goldstein at Bristol-Myers Squibb, and Dr. Mary Ann Ottinger at University of Maryland, personal communication). We suspect that some genetic and/or environmental factors altered this line after distribution by the University of California, Irvine. These findings provide guidance for the use of 3xTg-AD mice in therapeutic research.

Overall, this study demonstrated that 3xTg-AD mice show gender differences that may be relevant to human AD. Our findings suggest that both an increase in Abeta production and a decrease in Abeta degradation may contribute to the higher risk of AD in women.

4. Experimental procedures

4.1. *Animals and sampling*

We used 3xTg-AD mice (Oddo et al., 2003) generated by co-microinjection of mutant APP (K670M/N671L) and tau (P301L) transgenes under the control of Thy 1.2 promoter into mutant PS-1 (M146V) knock-in mice (Guo et al., 1999). 3xTg-AD mice were created by a group at the University California, Irvine, in collaboration with a group at the National Institute on Aging. The colony was established at Georgetown University using breeding pairs provided by the National Institute on Aging after homozygosity was confirmed by crossing with non-transgenic mice. All 3xTg-AD mice used in this study were bred and housed at the Georgetown University animal facility. Two other transgenic mouse lines were used for comparison purposes: Tg2576 APP transgenic mice (Taconic, Hudson, NY), the most widely used APP single transgenic mouse model, which expresses mutant APP (K670M/N671L) under the control of prion promoter (Hsiao et al., 1996), and PS/APP double transgenic mice (Holcomb et al., 1998) obtained by crossing Tg2576 with PS-1 transgenic mice (Duff et al., 1996). PS/APP mice were housed and the brains were collected at the Nathan Kline Institute for Psychiatric Research (Orangeburg, NY). This study has been reviewed and approved by the Georgetown University Animal Care and Use Committee.

For quantitative biochemical studies, we used male 3xTg-AD mice at 3 (3.3±0.0), 6 (6.0±0.2), 9 (8.7±0.1), 12 (12.2±0.1), 16 (16.1±0.1), 20 (20.2±0.3) and 23 (23±0.0) months of age (n=6 at each age), and female 3xTg-AD mice at 9 (9.1±0.4), 16 (16.1±0.1) and 23 (23.0±0.0) months of age (n=6 each). These mice were selected from at least two litters from different parents to avoid possible litter effects. Tg2576 APP transgenic male and female mice (n=5 each) were used at 4 (3.7±0.1) months of age. For histochemical analysis, we used additional mice: 3xTg-AD mice at 9 (9.1±0.2), 12 (11.7±0.1), 14 (14±0.2), 23 (22.7±0.3) and 28 (28±0.5) months of age (n=5 each), and PS/APP mice at 2 (2.5±0.0), 8 (7.6±0.0) and 13 (12.9±0.0) months of age (n=3, 2 and 2, respectively).

Mice were sacrificed by cervical dislocation to eliminate anesthesia-mediated tau phosphorylation (Planel et al., 2007), and the brains were quickly isolated. After the olfactory bulb and cerebellum were discarded, the hemi brain was snap-frozen in dry ice or immersion fixed in 4% paraformaldehyde in 0.1 M phosphate buffer, pH 7.4, for biochemical and histochemical analyses, respectively.

4.2. *Biochemical analysis of Abeta pathology*

Brains were homogenized in 10 volumes of 50 mM Tris–HCl buffer, pH 7.6, containing 250 mM sucrose and protease inhibitor cocktail (Sigma, St. Louis, MO). Soluble and total Abeta were extracted in 0.4% DEA and 70% FA, respectively, as previously described (Nishitomi et al., 2006; Takata et al., 2007; Sakaguchi et al., in press). Levels of full-length Abeta 1–40 and 1–42 were quantified using ELISAs developed by our group as previously described (Horikoshi et al., 2004; Matsuoka et al., 2008). Statistical significance was tested using t-tests or ANOVA followed by Bonferroni post-hoc tests (SPSS, Chicago, IL).

The DEA fraction and unfractionated crude brain homogenates were used to determine the levels of sAPPbeta and neprilysin, respectively. Samples were mixed with Laemmli buffer, run on a 4–15% gradient SDS-PAGE gel (BioRad, Hercules, CA) and the proteins were transferred to PVDF membrane (Millipore, Bedford, MA). The membrane was probed with mouse monoclonal antibodies against Swedish mutant sAPPbeta (clone 6A1, see below, 0.2 μg IgG/ml) or mouse neprilysin (0.2 μg IgG/ml, R&D Systems, Minneapolis, MN). The sAPPbeta Swedish antibody does not react with uncleaved APP or wild-type sAPPbeta (see below for sAPPbeta antibody characterization). The primary antibodies were detected by HRP-coupled anti-mouse IgG antibody (Jackson Immuno Research, West Grove, PA), and visualized with a chemiluminescence kit (Pierce). The protein bands were densitometrically analyzed (Quantity One, BioRad). Statistical significance was tested using t-tests or ANOVA (SPSS).

4.3. *Biochemical analysis of tau pathology*

Crude tau fraction was prepared as previously described (Matsuoka et al., 2008). Samples were run on a 4–15% gradient SDS-PAGE gel and the proteins were transferred to a PVDF membrane. The membrane was probed with a primary antibody: phosphorylated tau at Ser202 (clone AT8) (Biernat et al., 1992), Thr181 (clone AT270) (Greenberg and Davies, 1990) and Thr231 (clone AT180) (Greenberg and Davies, 1990) (all phosphorylated tau antibodies were used at 1 μg IgG/ml, Pierce Biotechnology, Rockford, IL). The primary antibodies were detected and quantified as described above.

4.4. *Histochemical analysis of Abeta pathology*

Brains were immersion fixed and sections were prepared as previously described (Matsuoka et al., 2001b). Sections were incubated with the primary antibodies in 100 mM phosphate buffered saline consisting of 0.3% Triton X-100 overnight. Sections were incubated with primary antibodies against Abeta (clone 82E1 (Horikoshi et al., 2004), Immuno-Biological Laboratories), APP/Abeta (clone 6E10 (Kosik et al., 1988), Signet Laboratories/Covance, Berkley, CA), and oligomeric Abeta (ADDL) (clone NU-1 (Lambert et al., 2007)). We used all primary antibodies at 1 μg IgG/ml. Primary antibodies were detected by a biotinylated secondary antibody (Vector Laboratories, Burlingame, CA) and then visualized using the ABC method (Vectastain, Vector Laboratories).

4.5. *Development and characterization of an antibody against Swedish-type sAPPbeta*

Mice (Balb/c, Charles River, Japan) were immunized with thyroglobulin-conjugated synthetic peptide corresponding to the C-terminus of Swedish mutant sAPPbeta (ISEVNL) or recombinant human APP N-terminal portion. After a series of immunizations, the spleen was isolated and spleen cells were fused with X63-Ag8 myeloma cells. We determined selectivity and sensitivity of these antibodies by microplate assay using the antigen and other recombinant proteins.

The full-length cDNA of human APP695 was amplified from human brain cDNA (Clontech, Mountain View, CA) using specific primers synthesized based on the published human APP cDNA sequence. To introduce the Swedish mutation, we used the following primers: Swe-sense: 5′-TCTGAAGTGAACTTGGATGCAGAA-3′, and Swe-antisense: 5′-TTCTGCATCCAAGTTCACTTCAGA-3′. The amplified products were digested with SalI and NotI, ligated into pGEX-6P-1 vector (Amersham Bioscience/GE Healthcare, Piscataway, NJ) and transformed into *Escherichia coli* JM109 cells. The sequence of the cloned wild-type and Swedish mutant APP cDNAs was confirmed. Wild-type sAPPbeta cDNA was amplified from APP695 cDNA by using following primers: Sal-APP: 5′-CGGTCGACTCGCGATGCTGCCCGGTTTGGC-3′ and sAPPbeta: 5′-GCGCGGCCGCCTACATCTTCACTTCAGAGAT-3′. Swedish sAPPbeta cDNA was also amplified from APP695 cDNA by using following primers: Sal-APP: 5′-CGGTCGACTCGCGATGCTGCCCGGTTTGGC-3′ and Swe-sAPPbeta-antisense: 5′-GCGCGGCCGCCTACAAGTTCACTTCAGAGATCTCCTCCG-3′. The amplified products were digested with SalI and NotI, ligated into pGEX-6P-1 vector and used to transform *E. coli* JM109 cells. The sequence of the cloned wild-type sAPPbeta and Swedish sAPPbeta cDNAs was confirmed.

The wild-type APP, wild-type sAPPbeta, Swedish APP and Swedish sAPPbeta cDNA in pGEX-6P-1 vector were transferred into pcDNA3.1(+) (Invitrogen, Carlsbad, CA). Then, APP and sAPPbeta cDNAs in pcDNA3.1(+) were transfected into COS-1cells by using FuGENE6 (Roche Diagnostics, Basel, Switzerland). Two days after transfection, cells were harvested by scraping with ice-cold 10 mM Tris buffer, pH 8.0, consisting of 1% NP-40, 150 mM NaCl and 1 mM EDTA. Cell lysates were run on a 10% SDS-PAGE gel and then transferred as described above. The membrane was probed with primary antibodies against the APP N-terminus or sAPPbeta (clone 10D1 or 6A1 at 5 or 1 μg IgG/ml, respectively).

Acknowledgments

We thank Ms. Hibiki Takenouchi, Department of Neurology, Georgetown University, for her technical assistance. Ms. Hibiki is a visiting student from Shiga University of Medical Science, Japan. We also thank Dr. Mary Ann Ottinger, University of Maryland, and Drs. Donna M. Barten and Margi Goldstein, Bristol-Myers Squibb for sharing their findings in the 3xTg-AD mouse colony maintained at their institute. Antibodies used for Abeta ELISA and Abeta immunostaining were generously provided by Dr. Noriaki Kinoshita at Immuno-Biological Laboratories. This study was supported by the National Institutes of Health (grants AG026478 and AG022455 to Y.M.), and the National Institute on Aging Intramural Research Program (MPM).

Disclosure statement: Northwestern University owns intellectual property concerning the use of globular Abeta oligomers (ADDLs) for Alzheimer's therapeutics and diagnostics which has been licensed to Acumen Pharmaceuticals. Dr. Klein is a co-founder of Acumen and a member of its Scientific Advisory Board.

REFERENCES

Barten, D.M., Guss, V.L., Corsa, J.A., Loo, A., Hansel, S.B., Zheng, M., Munoz, B., Srinivasan, K., Wang, B., Robertson, B.J., Polson, C.T., Wang, J., Roberts, S.B., Hendrick, J.P., Anderson, J.J., Loy, J.K., Denton, R., Verdoorn, T.A., Smith, D.W., Felsenstein, K.M., 2005. Dynamics of β-amyloid reductions in brain, cerebrospinal fluid, and plasma of β-amyloid precursor protein transgenic mice treated with a γ-secretase inhibitor. J. Pharmacol. Exp. Ther. 312, 635–643.

Biernat, J., Mandelkow, E.M., Schroter, C., Lichtenberg-Kraag, B., Steiner, B., Berling, B., Meyer, H., Mercken, M., Vandermeeren, A., Goedert, M., 1992. The switch of tau protein to an Alzheimer-like state includes the phosphorylation of two serine-proline motifs upstream of the microtubule binding region. EMBO J. 11, 1593–1597.

Braak, H., Braak, E., 1995. Staging of Alzheimer's disease-related neurofibrillary changes. Neurobiol. Aging 16, 271–278.

Brookmeyer, R., Gray, S., Kawas, C., 1998. Projections of Alzheimer's disease in the United States and the public health impact of delaying disease onset. Am. J. Public Health 88, 1337–1342.

Caccamo, A., Oddo, S., Sugarman, M.C., Akbari, Y., LaFerla, F.M., 2005. Age- and region-dependent alterations in Abeta-degrading enzymes: implications for Abeta-induced disorders. Neurobiol. Aging 26, 645–654.

Caccamo, A., Oddo, S., Tran, L.X., LaFerla, F.M., 2007. Lithium reduces tau phosphorylation but not A beta or working memory deficits in a transgenic model with both plaques and tangles. Am. J. Pathol. 170, 1669–1675.

Callahan, M.J., Lipinski, W.J., Bian, F., Durham, R.A., Pack, A., Walker, L.C., 2001. Augmented senile plaque load in aged female beta-amyloid precursor protein-transgenic mice. Am. J. Pathol. 158, 1173–1177.

Cummings, J.L., 2004. Alzheimer's disease. N. Engl. J. Med. 351, 56–67.

Duff, K., Eckman, C., Zehr, C., Yu, X., Prada, C.M., Perez-Tur, J., Hutton, M., Buee, L., Harigaya, Y., Yager, D., Morgan, D., Gordon, M.N., Holcomb, L., Refolo, L., Zenk, B., Hardy, J., Younkin, S., 1996. Increased amyloid-beta42(43) in brains of mice expressing mutant presenilin 1. Nature 383, 710–713.

Fukumoto, H., Cheung, B.S., Hyman, B.T., Irizarry, M.C., 2002. Beta-secretase protein and activity are increased in the neocortex in Alzheimer disease. Arch. Neurol. 59, 1381–1389.

Games, D., Adams, D., Alessandrini, R., Barbour, R., Berthelette, P., Blackwell, C., Carr, T., Clemens, J., Donaldson, T., Gillespie, F., 1995. Alzheimer-type neuropathology in transgenic mice overexpressing V717F beta-amyloid precursor protein. Nature 373, 523–527.

Gandy, S., Duff, K., 2000. Post-menopausal estrogen deprivation and Alzheimer's disease. Exp. Gerontol. 35, 503–511.

Gotz, J., Chen, F., Van Dorpe, J., Nitsch, R.M., 2001. Formation of neurofibrillary tangles in P301l tau transgenic mice induced by Abeta 42 fibrils. Science 293, 1491–1495.

Green, P.S., Bales, K., Paul, S., Bu, G., 2005. Estrogen therapy fails to alter amyloid deposition in the PDAPP model of Alzheimer's disease. Endocrinology 146, 2774–2781.

Greenberg, S.G., Davies, P., 1990. A preparation of Alzheimer paired helical filaments that displays distinct tau proteins by polyacrylamide gel electrophoresis. Proc. Natl. Acad. Sci. U. S. A. 87, 5827–5831.

Guo, Q., Fu, W., Sopher, B.L., Miller, M.W., Ware, C.B., Martin, G.M., Mattson, M.P., 1999. Increased vulnerability of hippocampal neurons to excitotoxic necrosis in presenilin-1 mutant knock-in mice. Nat. Med. 5, 101–106.

Hardy, J., Selkoe, D.J., 2002. The amyloid hypothesis of Alzheimer's disease: progress and problems on the road to therapeutics. Science 297, 353–356.

Henderson, V.W., Paganini-Hill, A., Miller, B.L., Elble, R.J., Reyes, P.F., Shoupe, D., McCleary, C.A., Klein, R.A., Hake, A.M., Farlow, M.R., 2000. Estrogen for Alzheimer's disease in women: randomized, double-blind, placebo-controlled trial. Neurology 54, 295–301.

Holcomb, L., Gordon, M.N., McGowan, E., Yu, X., Benkovic, S., Jantzen, P., Wright, K., Saad, I., Mueller, R., Morgan, D., Sanders, S., Zehr, C., O'Campo, K., Hardy, J., Prada, C.M., Eckman, C., Younkin, S., Hsiao, K., Duff, K., 1998. Accelerated Alzheimer-type phenotype in transgenic mice carrying both mutant amyloid precursor protein and presenilin 1 transgenes. Nat. Med. 4, 97–100.

Holsinger, R.M., McLean, C.A., Beyreuther, K., Masters, C.L., Evin, G., 2002. Increased expression of the amyloid precursor beta-secretase in Alzheimer's disease. Ann. Neurol. 51, 783–786.

Horikoshi, Y., Sakaguchi, G., Becker, A.G., Gray, A.J., Duff, K., Aisen, P.S., Yamaguchi, H., Maeda, M., Kinoshita, N., Matsuoka, Y., 2004. Development of Abeta terminal end-specific antibodies and sensitive ELISA for Abeta variant. Biochem. Biophys. Res. Commun. 319, 733–737.

Hsiao, K., Chapman, P., Nilsen, S., Eckman, C., Harigaya, Y., Younkin, S., Yang, F., Cole, G., 1996. Correlative memory deficits, Abeta elevation, and amyloid plaques in transgenic mice. Science 274, 99–102.

Huang, J., Guan, H., Booze, R.M., Eckman, C.B., Hersh, L.B., 2004. Estrogen regulates neprilysin activity in rat brain. Neurosci. Lett. 367, 85–87.

Hy, L.X., Keller, D.M., 2000. Prevalence of AD among whites: a summary by levels of severity. Neurology 55, 198–204.

Hyman, B.T., 1997. The neuropathological diagnosis of Alzheimer's disease: clinical–pathological studies. Neurobiol. Aging 18, S27–S32.

Iwata, N., Takaki, Y., Fukami, S., Tsubuki, S., Saido, T.C., 2002. Region-specific reduction of A beta-degrading endopeptidase, neprilysin, in mouse hippocampus upon aging. J. Neurosci. Res. 70, 493–500.

Iwata, N., Higuchi, M., Saido, T.C., 2005. Metabolism of amyloid-beta peptide and Alzheimer's disease. Pharmacol. Ther. 108, 129–148.

Kawas, C., Resnick, S., Morrison, A., Brookmeyer, R., Corrada, M., Zonderman, A., Bacal, C., Lingle, D.D., Metter, E., 1997. A prospective study of estrogen replacement therapy and the risk of developing Alzheimer's disease: the Baltimore Longitudinal Study of Aging. Neurology 48, 1517–1521.

Kosik, K.S., Orecchio, L.D., Binder, L., Trojanowski, J.Q., Lee, V.M., Lee, G., 1988. Epitopes that span the tau molecule are shared with paired helical filaments. Neuron 1, 817–825.

Lambert, M.P., Velasco, P.T., Chang, L., Viola, K.L., Fernandez, S., Lacor, P.N., Khuon, D., Gong, Y., Bigio, E.H., Shaw, P., De Felice, F.G., Krafft, G.A., Klein, W.L., 2007. Monoclonal antibodies that target pathological assemblies of Abeta. J. Neurochem. 100, 23–35.

Lazarov, O., Robinson, J., Tang, Y.P., Hairston, I.S., Korade-Mirnics, Z., Lee, V.M., Hersh, L.B., Sapolsky, R.M., Mirnics, K., Sisodia, S.S., 2005. Environmental enrichment reduces Abeta levels and amyloid deposition in transgenic mice. Cell 120, 701–713.

Lewis, J., McGowan, E., Rockwood, J., Melrose, H., Nacharaju, P., Van Slegtenhorst, M., Gwinn-Hardy, K., Paul Murphy, M., Baker, M., Yu, X., Duff, K., Hardy, J., Corral, A., Lin, W.L., Yen, S.H., Dickson, D.W., Davies, P., Hutton, M., 2000. Neurofibrillary tangles, amyotrophy and progressive motor disturbance in mice expressing mutant (P301L) tau protein. Nat. Genet. 25, 402–405.

Lewis, J., Dickson, D.W., Lin, W.L., Chisholm, L., Corral, A., Jones, G., Yen, S.H., Sahara, N., Skipper, L., Yager, D., Eckman, C., Hardy, J., Hutton, M., McGowan, E., 2001. Enhanced neurofibrillary degeneration in transgenic mice expressing mutant tau and APP. Science 293, 1487–1491.

Lindwall, G., Cole, R.D., 1984. Phosphorylation affects the ability of tau protein to promote microtubule assembly. J. Biol. Chem. 259, 5301–5305.

Matsuoka, Y., Picciano, M., La Francois, J., Duff, K., 2001a. Fibrillar beta-amyloid evokes oxidative damage in a transgenic mouse model of Alzheimer's disease. Neuroscience 104, 609–613.

Matsuoka, Y., Picciano, M., Malester, B., LaFrancois, J., Zehr, C., Daeschner, J.M., Olschowka, J.A., Fonseca, M.I., O'Banion, M.K., Tenner, A.J., Lemere, C.A., Duff, K., 2001b. Inflammatory responses to amyloidosis in a transgenic mouse model of Alzheimer's disease. Am. J. Pathol. 158, 1345–1354.

Matsuoka, Y., Jouroukhin, Y., Gray, A.J., Ma, L., Hirata-Fukae, C., Li, H.-F., Feng, L., Lecanu, L., Walker, B.R., Planel, E., Arancio, O., Gozes, I., Aisen, P.S., 2008. A neuronal microtubule-interacting agent, NAPVSIPQ, reduces tau pathology and enhances cognitive function in a mouse model of Alzheimer's disease. J. Pharmacol. Exp. Ther. 325, 146–153.

McDowell, I., 2001. Alzheimer's disease: insights from epidemiology. Aging (Milano.) 13, 143–162.

McGowan, E., Eriksen, J., Hutton, M., 2006. A decade of modeling Alzheimer's disease in transgenic mice. Trends Genet. 22, 281–289.

Mukai, H., Takata, N., Ishii, H.T., Tanabe, N., Hojo, Y., Furukawa, A., Kimoto, T., Kawato, S., 2006. Hippocampal synthesis of estrogens and androgens which are paracrine modulators of synaptic plasticity: synaptocrinology. Neuroscience 138, 757–764.

Mulnard, R.A., Cotman, C.W., Kawas, C., van Dyck, C.H., Sano, M., Doody, R., Koss, E., Pfeiffer, E., Jin, S., Gamst, A., Grundman, M.,

Thomas, R., Thal, L.J., 2000. Estrogen replacement therapy for treatment of mild to moderate Alzheimer disease: a randomized controlled trial. Alzheimer's Disease Cooperative Study. JAMA 283, 1007–1015.

Nishitomi, K., Sakaguchi, G., Horikoshi, Y., Gray, A.J., Maeda, M., Hirata-Fukae, C., Becker, A.G., Hosono, M., Sakaguchi, I., Minami, S.S., Nakajima, Y., Li, H.F., Takeyama, C., Kihara, T., Ota, A., Wong, P.C., Aisen, P.S., Kato, A., Kinoshita, N., Matsuoka, Y., 2006. BACE1 inhibition reduces endogenous Abeta and alters APP processing in wild-type mice. J. Neurochem. 99, 1555–1563.

Oddo, S., Caccamo, A., Shepherd, J.D., Murphy, M.P., Golde, T.E., Kayed, R., Metherate, R., Mattson, M.P., Akbari, Y., LaFerla, F.M., 2003. Triple-transgenic model of Alzheimer's disease with plaques and tangles. Intracellular abeta and synaptic dysfunction. Neuron 39, 409–421.

Oddo, S., Billings, L., Kesslak, J.P., Cribbs, D.H., LaFerla, F.M., 2004. Abeta immunotherapy leads to clearance of early, but not late, hyperphosphorylated tau aggregates via the proteasome. Neuron 43, 321–332.

Planel, E., Richter, K.E., Nolan, C.E., Finley, J.E., Liu, L., Wen, Y., Krishnamurthy, P., Herman, M., Wang, L., Schachter, J.B., Nelson, R.B., Lau, L.F., Duff, K.E., 2007. Anesthesia leads to tau hyperphosphorylation through inhibition of phosphatase activity by hypothermia. J. Neurosci. 27, 3090–3097.

Ramsden, M., Kotilinek, L., Forster, C., Paulson, J., McGowan, E., SantaCruz, K., Guimaraes, A., Yue, M., Lewis, J., Carlson, G., Hutton, M., Ashe, K.H., 2005. Age-dependent neurofibrillary tangle formation, neuron loss, and memory impairment in a mouse model of human tauopathy (P301L). J. Neurosci. 25, 10637–10647.

Roberson, E.D., Scearce-Levie, K., Palop, J.J., Yan, F., Cheng, I.H., Wu, T., Gerstein, H., Yu, G.Q., Mucke, L., 2007. Reducing endogenous tau ameliorates amyloid beta-induced deficits in an Alzheimer's disease mouse model. Science 316, 750–754.

Sakaguchi, G., Aisen, P.S., Matsuoka, Y., in press. Testing secretase inhibitors using in vivo models. In: Recent advances in the biology of secretases, key proteases in Alzheimer disease (ed. Araki, W.).

SantaCruz, K., Lewis, J., Spires, T., Paulson, J., Kotilinek, L., Ingelsson, M., Guimaraes, A., DeTure, M., Ramsden, M., McGowan, E., Forster, C., Yue, M., Orne, J., Janus, C., Mariash, A., Kuskowski, M., Hyman, B., Hutton, M., Ashe, K.H., 2005. Tau suppression in a neurodegenerative mouse model improves memory function. Science 309, 476–481.

Takata, K., Hirata-Fukae, C., Becker, A.G., Chishiro, S., Gray, A.J., Nishitomi, K., Franz, A.H., Sakaguchi, G., Kato, A., Mattson, M.P., LaFerla, F.M., Aisen, P.S., Kitamura, Y., Matsuoka, Y., 2007. Deglycosylated anti-amyloid beta antibodies reduce microglial phagocytosis and cytokine production while retaining the capacity to induce amyloid beta sequestration. Eur. J Neurosci. 26, 2458–2468.

Tang, M.X., Jacobs, D., Stern, Y., Marder, K., Schofield, P., Gurland, B., Andrews, H., Mayeux, R., 1996. Effect of oestrogen during menopause on risk and age at onset of Alzheimer's disease. Lancet 348, 429–432.

Trojanowski, J.Q., Lee, V.M., 1995. Phosphorylation of paired helical filament tau in Alzheimer's disease neurofibrillary lesions: focusing on phosphatases. FASEB J. 9, 1570–1576.

varez-de-la-Rosa, M., Silva, I., Nilsen, J., Perez, M.M., Garcia-Segura, L.M., Avila, J., Naftolin, F., 2005. Estradiol prevents neural tau hyperphosphorylation characteristic of Alzheimer's disease. Ann. N.Y. Acad. Sci. 1052, 210–224.

Walsh, D.M., Tseng, B.P., Rydel, R.E., Podlisny, M.B., Selkoe, D.J., 2000. The oligomerization of amyloid beta-protein begins intracellularly in cells derived from human brain. Biochemistry 39, 10831–10839.

Walsh, D.M., Klyubin, I., Fadeeva, J.V., Cullen, W.K., Anwyl, R., Wolfe, M.S., Rowan, M.J., Selkoe, D.J., 2002. Naturally secreted oligomers of amyloid beta protein potently inhibit hippocampal long-term potentiation in vivo. Nature 416, 535–539.

Wang, P.N., Liao, S.Q., Liu, R.S., Liu, C.Y., Chao, H.T., Lu, S.R., Yu, H.Y., Wang, S.J., Liu, H.C., 2000. Effects of estrogen on cognition, mood, and cerebral blood flow in AD: a controlled study. Neurology 54, 2061–2066.

Waring, S.C., Rocca, W.A., Petersen, R.C., O'Brien, P.C., Tangalos, E.G., Kokmen, E., 1999. Postmenopausal estrogen replacement therapy and risk of AD: a population-based study. Neurology 52, 965–970.

Yang, L.B., Lindholm, K., Yan, R., Citron, M., Xia, W., Yang, X.L., Beach, T., Sue, L., Wong, P., Price, D., Li, R., Shen, Y., 2003. Elevated beta-secretase expression and enzymatic activity detected in sporadic Alzheimer disease. Nat. Med. 9, 3–4.

Zandi, P.P., Carlson, M.C., Plassman, B.L., Welsh-Bohmer, K.A., Mayer, L.S., Steffens, D.C., Breitner, J.C., 2002. Hormone replacement therapy and incidence of Alzheimer disease in older women: the Cache County Study. JAMA 288, 2123–2129.

Zhao, J., Fu, Y., Yasvoina, M., Shao, P., Hitt, B., O'Connor, T., Logan, S., Maus, E., Citron, M., Berry, R., Binder, L., Vassar, R., 2007. Beta-site amyloid precursor protein cleaving enzyme 1 levels become elevated in neurons around amyloid plaques: implications for Alzheimer's disease pathogenesis. J. Neurosci. 27, 3639–3649.

Zheng, H., Xu, H., Uljon, S.N., Gross, R., Hardy, K., Gaynor, J., LaFrancois, J., Simpkins, J., Refolo, L.M., Petanceska, S., Wang, R., Duff, K., 2002. Modulation of A(beta) peptides by estrogen in mouse models. J. Neurochem. 80, 191–196.

BIOCHEMISTRY
including biophysical chemistry & molecular biology

Article

Amyloidogenic Processing of Amyloid Precursor Protein: Evidence of a Pivotal Role of Glutaminyl Cyclase in Generation of Pyroglutamate-Modified Amyloid-#

Holger Cynis, Eike Scheel, Takaomi C. Saido, Stephan Schilling, and Hans-Ulrich Demuth

Biochemistry, **2008**, 47 (28), 7405-7413• DOI: 10.1021/bi800250p • Publication Date (Web): 21 June 2008

More About This Article

Additional resources and features associated with this article are available within the HTML version:

- Supporting Information
- Access to high resolution figures
- Links to articles and content related to this article
- Copyright permission to reproduce figures and/or text from this article

View the Full Text HTML

Amyloidogenic Processing of Amyloid Precursor Protein: Evidence of a Pivotal Role of Glutaminyl Cyclase in Generation of Pyroglutamate-Modified Amyloid-β[†]

Holger Cynis,[‡] Eike Scheel,[‡] Takaomi C. Saido,[§] Stephan Schilling,*[,‡] and Hans-Ulrich Demuth[‡]

Probiodrug AG, Weinbergweg 22, 06120 Halle/Saale, Germany, and Laboratory for Proteolytic Neuroscience, RIKEN Brain Science Institute, 2-1 Hirosawa, Wako, Saitama 351-0198, Japan

Received February 12, 2008; Revised Manuscript Received April 29, 2008

ABSTRACT: Compelling evidence suggests that N-terminally truncated and pyroglutamyl-modified amyloid-β (Aβ) peptides play a major role in the development of Alzheimer's disease. Posttranslational formation of pyroglutamic acid (pGlu) at position 3 or 11 of Aβ implies cyclization of an N-terminal glutamate residue rendering the modified peptide degradation resistant, more hydrophobic, and prone to aggregation. Previous studies using artificial peptide substrates suggested the potential involvement of the enzyme glutaminyl cyclase in generation of pGlu-Aβ. Here we show that glutaminyl cyclase (QC) catalyzes the formation of A$\beta_{3(pE)-40/42}$ after amyloidogenic processing of APP in two different cell lines, applying specific ELISAs and Western blotting based on urea−PAGE. Inhibition of QC by the imidazole derivative PBD150 led to a blockage of A$\beta_{3(pE)-42}$ formation. Apparently, the QC-catalyzed formation of N-terminal pGlu is favored in the acidic environment of secretory compartments, which is also supported by double-immunofluorescence labeling of QC and APP revealing partial colocalization. Finally, initial investigations focusing on the molecular pathway leading to the generation of truncated Aβ peptides imply an important role of the amino acid sequence near the β-secretase cleavage site. Introduction of a single-point mutation, resulting in an amino acid substitution, APP(E599Q), i.e., at position 3 of Aβ, resulted in significant formation of A$\beta_{3(pE)-40/42}$. Introduction of the APP KM595/596NL "Swedish" mutation causing overproduction of Aβ, however, surprisingly diminished the concentration of A$\beta_{3(pE)-40/42}$. The study provides new cell-based assays for the profiling of small molecule inhibitors of QC and points to conspicuous differences in processing of APP depending on sequence at the β-secretase cleavage site.

Alzheimer's disease (AD)[1] has emerged as the major cause of dementia in the developed world, affecting approximately 20−25 million patients (*1*). Neurofibrillary tangles and senile plaques, which are found *post mortem* in cortical and hippocampal brain sections of AD patients, represent the major histopathological hallmarks of the disease. According to the amyloid cascade hypothesis, amyloid-β (Aβ) peptides, the primary components of senile plaques, are key for the development of the disease (*1*, *2*). These A$\beta_{40/42}$ peptides are liberated sequentially by proteolysis of the amyloid precursor protein (APP) by β- and γ-secretases (*3*, *4*). Aβ undergoes a high level of turnover within the brain, and its impaired degradation is presumed to be the primary cause of Aβ deposition (*1*, *5*, *6*).

It has been shown that N-terminal variants of Aβ are abundant in human amyloid deposits and soluble Aβ. Modifications affect the aspartic acids at positions 1 and 7, which are isomerized or racemized (*7–10*), or the glutamic acid residues at position 3 and 11, which are found to be cyclized into pyroglutamic acid (pGlu) after liberation by peptidases. In this regard, the most prominent N-terminal variant has been identified as A$\beta_{3(pE)-42}$ (*7*, *11–15*). The A$\beta_{3/11(pE)-40/42}$ peptides are suggested to play a crucial role in the development of AD, since deposition occurs early in AD and A$\beta_{3(pE)-40/42}$ exhibited pronounced toxicity in neuronal and glial cell cultures (*14*, *16*). In addition, pGlu-modified Aβ species exhibit an up to 250-fold accelerated initial rate of aggregation compared to that of unmodified Aβ, suggesting these peptides as potential seeding species for neurotoxic aggregate formation in vivo (*17*, *18*). Importantly, in healthy and pathologically aged brains, profound plaque pathology without signs of dementia has been observed, which is accompanied by A$\beta_{3(pE)-42}$ at low levels (*19*). Finally, the occurrence of intracellular N-truncated Aβ species correlates with hippocampal neuron loss in a mouse model (*20*), supporting a decisive role of pGlu-Aβ in the development of AD.

Human glutaminyl cyclase (QC) was recently shown to convert N-terminal glutamate residues into pyroglutamic acid in vitro (*21*, *22*). In the study presented here, the glutam(in)yl cyclase-mediated pGlu formation was analyzed in detail in cultures of human cell lines HEK293 and LNZ308. The aim of the work was to investigate the generation of A$\beta_{3(pE)-42}$ in

[†] This work was supported by a grant from the German Federal Department of Education, Science and Technology, BMBF 0313185 to H.-U.D.

* To whom correspondence should be addressed: Probiodrug AG, Weinbergweg 22, 06120 Halle, Germany. Telephone: +49 (345) 5559900. Fax: +49 (345) 5559901. E-mail: stephan.schilling@probiodrug.de.

[‡] Probiodrug AG.

[§] RIKEN Brain Science Institute.

[1] Abbreviations: Aβ, β-amyloid peptide; AD, Alzheimer's disease; APP, amyloid precursor protein; ELISA, enzyme-linked immunosorbent assay; FBD, familial British dementia; FDD, familial Danish dementia; H-Gln-βNA, glutamine β-naphthylamine; PAGE, polyacrylamide gel electrophoresis; pGlu, pyroglutamic acid; QC, glutaminyl cyclase; TMB, tetramethylbenzidine; WT, wild type.

10.1021/bi800250p CCC: $40.75
Published on Web 06/21/2008

Scheme 1: APP695 constructs used in this study, including APP(WT), APP(Swedish) (KM595/596NL), APP(London) (V642I), and APP(Swedish/London) (KM595/596NL, V642I)[a]

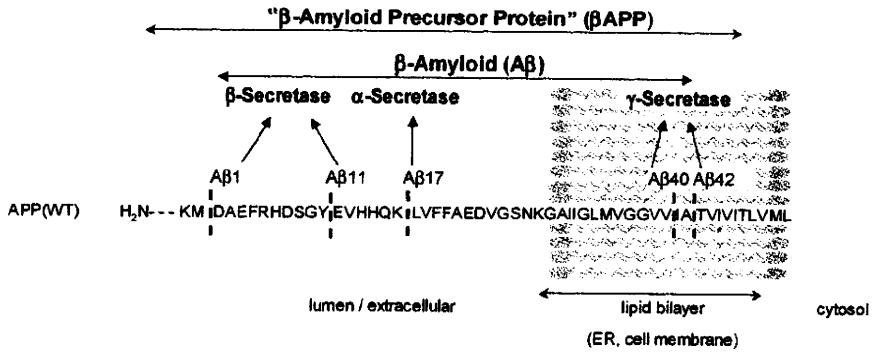

APP(Swedish)	H2N- - - NL DAEFRHDSGY EVHHQK LVFFAEDVGSNKGAIIGLMVGGV V IA TVIVITLVML
APP(London)	H2N- - -KM DAEFRHDSGY EVHHQK LVFFAEDVGSNKGAIIGLMVGGV V IA TVI I TLVML
APP(Swedish/London)	H2N- - - NL DAEFRHDSGY EVHHQK LVFFAEDVGSNKGAIIGLMVGGV V IA TVI I ITLVML
APP(WT) (N3Q)	H2N- - -KM DAQFRHDSGY EVHHQK LVFFAEDVGSNKGAIIGLMVGGV V IA TVIVITLVML
APP(NLE)	H2N- - - NL - - EFRHDSGY EVHHQK LVFFAEDVGSNKGAIIGLMVGGV V IA TVI I ITLVML
APP(NLQ)	H2N- - - NL - - QFRHDSGY EVHHQK LVFFAEDVGSNKGAIIGLMVGGV V IA TVI I ITLVML

[a] All APP constructs were also tested, containing additionally a N3Q mutation (E599Q). For example, APP(WT) (N3Q) is shown. For investigating glutamate cyclization by human glutaminyl cyclase, the constructs APP(NLE) (KM595/596NL, ΔD597, ΔA598, V642I) and APP(NLQ) (KM595/596NL, ΔD597, ΔA598, E599Q, V642I) were used.

mammalian cell culture by expression of APP and QC to show whether QC is capable of generating $A\beta_{3(pE)-42}$ following amyloidogenic processing of APP. The results, thus, should provide new cell-based screening systems for small molecule QC inhibitors and validate QC inhibition as a strategy for preventing pGlu-Aβ formation.

EXPERIMENTAL PROCEDURES

Peptides. Aβ peptides were purchased from AnaSpec (San Jose, CA) or synthesized as described previously (*17*).

Vectors. The cDNAs of human APP695(Swedish/London), APP(NLE), and APP(NLQ) was generated as described previously (*22, 23*). The E599Q point mutation was introduced into the FAD- and WT-containing APP cDNAs. The cDNAs were ligated into the *Not*I site of vector pcDNA 3.1(+) (Invitrogen) (Scheme 1). Additionally, the human QC was inserted into vector pcDNA 3.1(+) using *Hin*dIII and *Not*I restriction sites. For generation of a human QC−EGFP fusion protein, the enhanced green fluorescent protein was inserted into the *Xho*I site of vector pcDNA 3.1(+) and subsequently fused to human QC cDNA lacking the stop codon using the *Hin*dIII and *Not*I sites. All constructs were confirmed by sequencing and isolated for cell culture purposes using the EndoFree Plasmid Maxi Kit (Qiagen).

Cell Culture and Transfection. Human embryonic kidney cells (HEK293) and human glioma cell line LNZ308 were cultured in DMEM (10% FBS) in a humidified atmosphere of 5% CO_2 at 37 °C. Cells were transfected with APP695 variants with Lipofectamine2000 (Invitrogen), essentially as described previously (*22*). The next day, cells were either analyzed for APP expression using Western blotting and immunohistochemistry or incubated for 24 h in assay medium (DMEM, without phenol red, without FBS). The supernatant was collected and readily mixed with Complete Mini protease inhibitor cocktail (Roche) supplemented with additional 1 mM AEBSF (Roth) to prevent unspecific degradation by proteases. The samples were stored at −80 °C until the assay.

Concentration of Aβ Peptides. Prior to Western blot analysis of Aβ, the conditioned media were collected. Aβ was concentrated using Hydrosart centricons (Sartorius) with a 1 kDa cutoff. For immunoprecipitation, monoclonal antibody 4G8 (Chemicon), detecting total Aβ, was added to the cell culture medium and the mixture incubated under continuous shaking for 24 h at 4 °C. The next day, sheep anti-mouse IgG dynalbeads (Invitrogen) were added to the solution and the mixture was incubated for an additional 24 h at 4 °C. Afterward, Aβ peptides were dislodged by boiling in urea−PAGE gel buffer for 5 min and analyzed by Western blotting. For ELISA detection, the beads were incubated in a methanol/formic acid solution for 1 h. The supernatant was neutralized by addition of 200 mM phosphate buffer (pH 8.0) and EIA ELISA diluent buffer (IBL-Hamburg) and subsequently probed on the desired ELISA plate.

Western Blot Analysis. The detection of APP was performed applying Tris-glycine−PAGE as described previously (*22*). The electrophoretic separation of N-terminally modified Aβ peptides was carried out using 15% urea−PAGE gels (*24*). Proteins were transferred to a nitrocellulose membrane under semidry conditions. Subsequently, the membrane was blocked using 3% (w/v) dry milk in TBS-T [20 mM Tris-HCl (pH 7.5), 500 mM NaCl, and 0.05% (v/v) Tween 20]. APP and Aβ were detected using a polyclonal anti-APP antibody (Cell Signaling) and monoclonal anti-Aβ(1−16) antibody 6E10 (Chemicon), respectively. Pyroglutamyl-modified Aβ was detected applying antibody 8E1 (IBL-Hamburg). For visualization, blot membranes were incubated with secondary antibodies (anti-rabbit for APP and anti-mouse for Aβ), both conjugated with horseradish peroxidase (Cell Signaling) in TBS-T containing 5% (w/v) dry milk, and subsequently developed using the SuperSignal West Pico System (Pierce) according to the manufacturer's protocol.

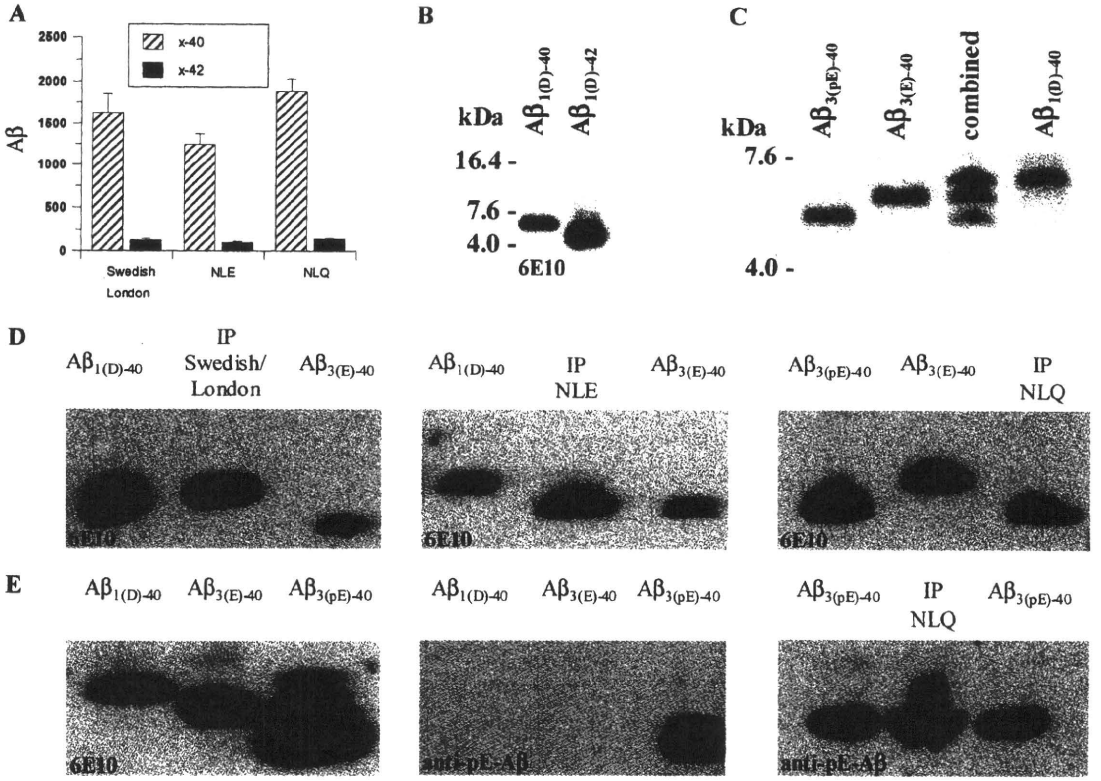

FIGURE 1: (A) Analysis of $A\beta_{x\text{-}40}$ (hatched bars) and $A\beta_{x\text{-}42}$ (black bars) secreted by HEK293 cells, which were transfected with APP(Swedish/London), APP(NLE), and APP(NLQ) using an ELISA detecting either $A\beta_{x\text{-}40}$ or $A\beta_{x\text{-}42}$ (total Aβ). The Aβ concentration was normalized to cell count (picograms per milliliter per 1×10^6 cells) ($n = 6$). (B) Urea−PAGE followed by Western blot analysis of 10 ng of $A\beta_{1(D)\text{-}40}$ in comparison to 10 ng of $A\beta_{1(D)\text{-}42}$ standard peptides. (C) Urea−PAGE followed by Coomassie staining of different N-terminal variants of $A\beta_{40}$ (3 μg each). (D) Western blot of Aβ species secreted by HEK293 cells expressing APP(Swedish/London), APP(NLE), and APP(NLQ) in comparison to 10 ng of standard Aβ peptides. (E) In addition, an antibody specific for $A\beta_{3(pE)\text{-}x}$ was implemented, showing the generation of $A\beta_{3(pE)\text{-}40}$ after expression of APP(NLQ), compared to $A\beta_{3(pE)\text{-}40}$ standard peptides (10 ng).

Immunohistochemistry. Cells were washed twice with D-PBS (Invitrogen) and fixed using ice-cold methanol for 10 min, followed by three washing steps using D-PBS for 10 min at room temperature. For staining of the Golgi complex, HEK293 cells were incubated with rabbit anti-mannosidase II polyclonal antibody (Chemicon), applying a 1:50 dilution of the antibody in D-PBS at room temperature for 3 h. For APP and Aβ staining, HEK293 cells were incubated at room temperature with mouse anti-β-amyloid monoclonal antibody 6E10 (Calbiochem) for 3 h using a 1:50 dilution of the antibody in D-PBS. Subsequently, the cells were washed three times with D-PBS for 10 min. The immunostained Golgi complex and APP were tagged by applying IgG secondary antibodies, which were conjugated with Rhodamin-RedX (Dianova). The samples were incubated at room temperature in the dark for 45 min. Afterward, cells were washed three times with D-PBS for 5 min at room temperature. Finally, the fixed and stained samples were mounted with citiflour and covered with a microscope slide. The cells were observed with oil immersion using a confocal laser scanning microscope (Carl-Zeiss).

Quantification of Aβ Peptides and QC Activity. Glutaminyl cyclase activity was measured using the substrate H-Gln-βNA as described previously (*25*). The assay reaction was started by addition of the QC-containing cell culture supernatant and evaluated using a Novostar reader for microplates (BMG-Labtechnologies). QC activity was determined from a standard curve of β-naphthylamine under assay conditions. $A\beta_{40}$ and $A\beta_{42}$ concentrations were determined using specific sandwich ELISAs detecting total $A\beta_{x\text{-}40}$ and $A\beta_{x\text{-}42}$, full-length $A\beta_{1(D)\text{-}40}$ and $A\beta_{1(D)\text{-}42}$, or the N-terminally pyroglutamated variants $A\beta_{3(pE)\text{-}40}$ and $A\beta_{3(pE)\text{-}42}$ (all IBL-Hamburg) according to the manufacturer's instructions.

Investigation of Intracellular pGlu Formation. HEK293 cells were transfected with vector APP(NLE) alone or in combination with a vector encoding the native human QC. Additionally, HEK293 cells were transfected with APP(NLE) alone, and recombinant human QC was added to the cell culture medium. After 24 h, samples were collected and the Aβ concentration was determined using ELISAs.

RESULTS

Generation of $A\beta_{3(pE)\text{-}40/42}$ Peptides in Cell Culture. On the basis of several different APP constructs (Scheme 1), the N- and C-terminal heterogeneity of Aβ peptides generated by HEK293 cells was assessed. Expression of all APP variants led to a significant increase in the $A\beta_{x\text{-}40}$ and $A\beta_{x\text{-}42}$ concentration (not shown), which was in good agreement with previous findings (*26, 27*), suggesting that the HEK293 expression system is well-suited for analysis of $A\beta_{x\text{-}40/42}$ formation. The Aβ concentrations were negligible in conditioned media of untransfected or mock transfected cells.

To prove QC-mediated pGlu-Aβ formation occurred after amyloidogenic processing of APP, we expressed APP(Swedish/London) and its modified variants APP(NLE) and

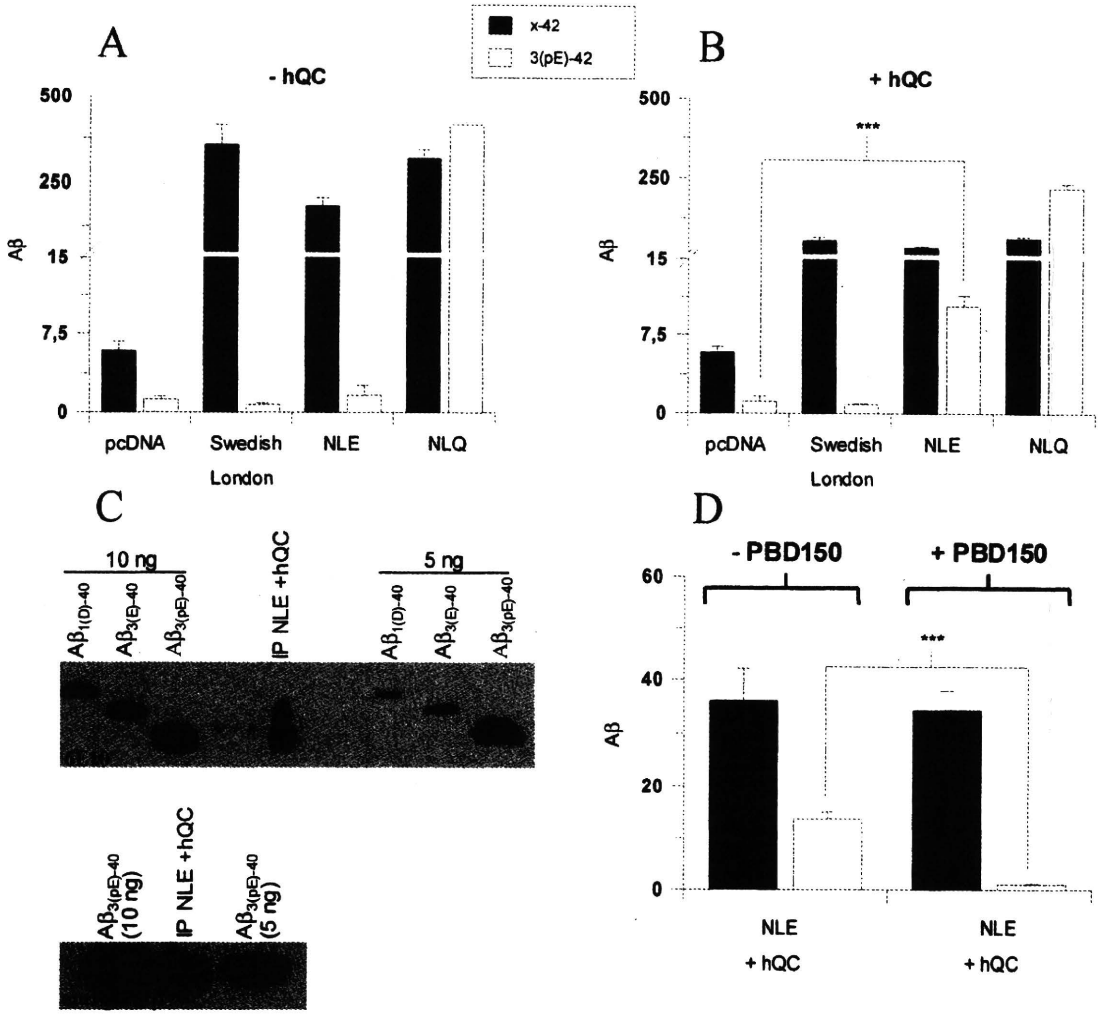

FIGURE 2: Analysis of pGlu formation after expression of vectors pcDNA, APP(Swedish/London), APP(NLE), and APP(NLQ) in HEK293 cells using an ELISA in the absence (A) or presence (B) of cotransfection with human QC. Aβ concentrations were normalized to cell count (picograms per milliliter per 1×10^6 cells) (asterisks, $P < 0.001$; Student's t test; $n = 3$). (C) QC-dependent pGlu formation of APP(NLE) was corroborated using Western blot analysis detecting total-Aβ (6E10) or pGlu-modified Aβ (anti-pE-Aβ) (application in comparison to standard Aβ peptides). (D) The formation of $A\beta_{3(pE)-42}$ after cotransfection of APP(NLE) with human QC was inhibited by application of the QC-specific inhibitor PBD150 (10 μM). Aβ concentrations were normalized to cell count (picograms per milliliter per 1×10^6 cells) (asterisks, $P < 0.001$; Student's t test; $n = 6$).

APP(NLQ) (Scheme 1) in HEK293 cells. The processing of the latter constructs should result in rapid liberation of $A\beta_{3(E)-40/42}$ and $A\beta_{3(Q)-40/42}$, i.e., precursors of $A\beta_{3(pE)-40/42}$. The expression of APP(Swedish/London), APP(NLE), and APP(NLQ) resulted in comparable $A\beta_{x-40/42}$ concentrations in the cell culture supernatant (Figure 1A). In addition, the secreted Aβ peptides were analyzed using urea−PAGE according to the method of Kalfki et al. (*24*), followed by Western blot analysis. In agreement with the earlier observations using urea−PAGE, $A\beta_{1(D)-42}$ migrates faster than $A\beta_{1(D)-40}$ (Figure 1B). Furthermore, the method enables the separation of $A\beta_{1(D)-40}$, $A\beta_{3(E)-40}$, and $A\beta_{3(pE)-40}$ (Figure 1C). According to the Western blot analysis, the expression of APP(Swedish/London) led to Aβ peptides starting with aspartate 1 [$A\beta_{1(D)-40/42}$]. In contrast, transfection of APP(NLE) resulted primarily in $A\beta_{3(E)-40/42}$, as revealed by the faster migration in urea−PAGE, whereas the transfection of APP(NLQ) exclusively generated $A\beta_{3(pE)-40/42}$ (Figure 1D). The dominant formation of $A\beta_{3(pE)}$ by expression of APP(NLQ) is most likely caused by rapid QC-catalyzed cyclization of $A\beta_{3(Q)-40/42}$, possibly accompanied by spontaneous cyclization of glutamine (Figure 1E) (*22*, *23*). In conclusion, the results suggest that β- and γ-secretase appropriately process the APP variants APP(NLE) and APP(NLQ).

$A\beta_{3(pE)}$ Formation Is Catalyzed by QC. Since the expression of APP(Swedish/London) and its derivatives APP(NLE) and APP(NLQ) led to the secretion of Aβ peptides starting with distinct N-terminal amino acids (aspartic acid, glutamic acid, or glutamine), these vectors were analyzed for $A\beta_{x-40/42}$ and $A\beta_{3(pE)-40/42}$ generation after transfection into HEK293 cells. Again, expression of APP(Swedish/London), APP(NLE), and APP(NLQ) resulted in generation of $A\beta_{x-40/42}$ peptides, but significant $A\beta_{3(pE)-40/42}$ formation could be detected only in the case of APP(NLQ), which is catalyzed by endogenous QC, present in HEK293 cells (*22*) (Figures 1E and 2A). However, formation of $A\beta_{3(pE)-42}$ was observed after cotransfection of APP(NLE) with human QC (Figure 2B). This finding was further corroborated by Western blot analysis after immunoprecipitation of Aβ peptides from the cell culture supernatant of HEK293 cells coexpressing

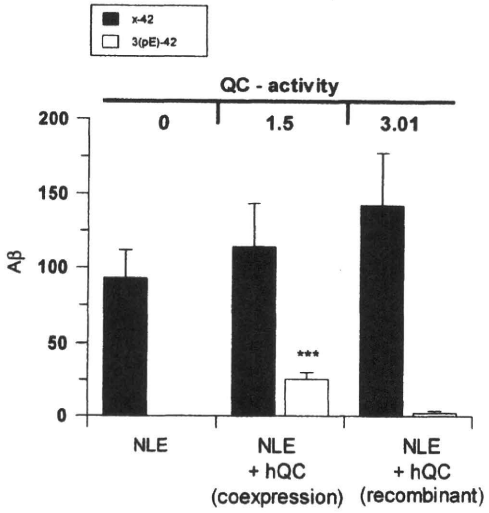

FIGURE 3: Determination of QC-dependent intracellular and extracellular $A\beta_{3(pE)-42}$ formation in HEK293 cells. Expression of APP(NLE) in the absence or presence of coexpression with native human QC or expression of APP(NLE) and subsequent application of recombinant human QC to the cell culture medium. Determination of the amount of $A\beta_{x-42}$ (black bars) and $A\beta_{3(pE)-42}$ (white bars) by an ELISA. QC activity (in micromolar per minute per 1 $\times 10^6$ cells) was measured using a fluorescence assay (asterisks, $P < 0.001$; Student's t test; $n = 6$).

APP(NLE) and human QC (Figure 2C). The detection of $A\beta_{3(pE)-42}$ after cotransfection of APP(NLE) and human QC typically resulted in 5−20% pGlu formation at the N-terminus of Aβ (Figure 2B, replication not shown). Interestingly, if the Aβ peptides where immunoprecipitated, the $A\beta_{3(pE)}$ band was more prominent than the unmodified $A\beta_{3(E)}$ signal, when using antibody 6E10 for detection. However, when the anti-pE-Aβ antibody was applied, a rather weak pGlu-Aβ signal was obtained (Figure 2C).

In an accompanying experiment, the efficacy of the QC inhibitor PBD150 in suppressing the formation of $A\beta_{3(pE)}$ was evaluated. Therefore, APP(NLE) and human QC were coexpressed in the absence and presence of 10 μM PBD150. The inhibitor did not affect the secretion of total $A\beta_{x-42}$. However, the extent of $A\beta_{3(pE)-42}$ generation was significantly lower, when PBD150 was applied (Figure 2D).

QC-Dependent $A\beta_{3(pE)}$ Formation Is Favored Intracellularly. Previous investigations of the pH dependency of QC-catalyzed cyclization of glutamic acid in vitro revealed an optimum under mildly acidic conditions. Localizing the environment under which the cyclization occurs in the cell-based system was another goal. Cotransfection of APP(NLE) with human QC led to N-terminal cyclization of glutamate and, because of secretion of the enzyme, to an increased QC activity within the cell culture medium (not shown). Therefore, there was a need for elucidation of whether an intracellular colocalization of human QC and APP(NLE) was required for $A\beta_{3(pE)}$ formation or the QC activity within the medium was responsible. The APP(NLE) construct was expressed either singly or in combination with human QC. In parallel samples, recombinant human QC (*28*) was applied to the culture medium of cells expressing APP(NLE) to clarify whether extracellular QC activity contributes to the glutamate cyclization. As expected, the single expression of APP(NLE) led only to the detection of $A\beta_{x-42}$. In contrast, cotransfection of APP(NLE) with human QC resulted in

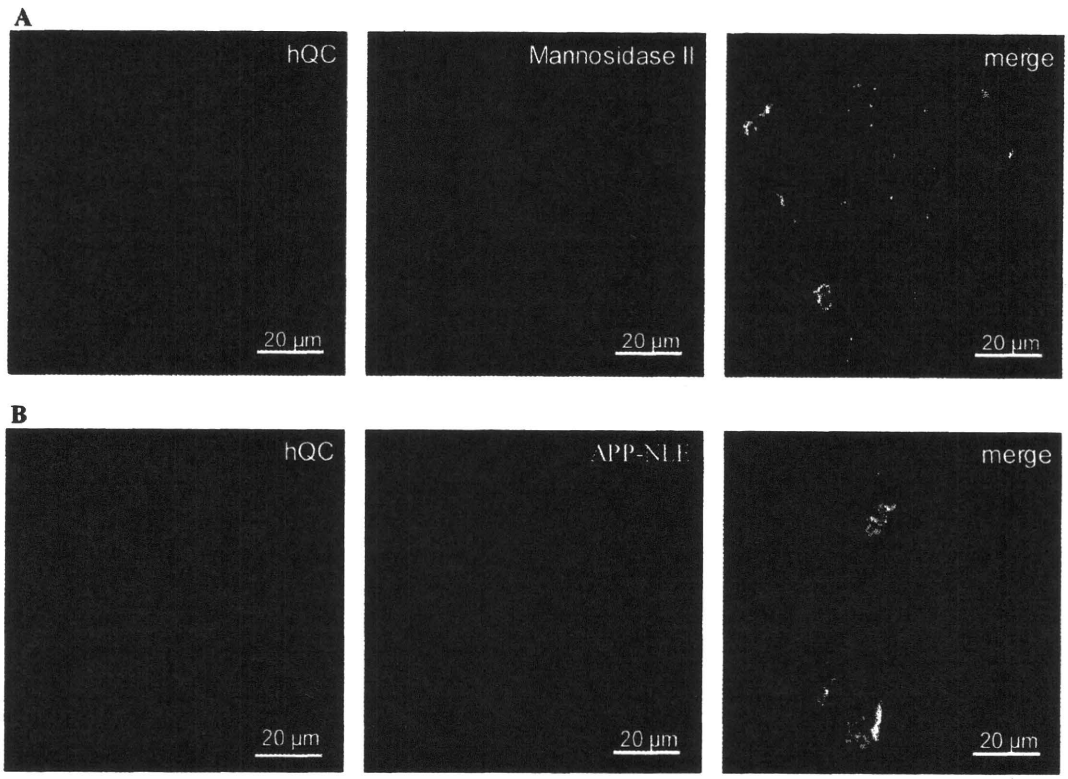

FIGURE 4: (A) Immunohistochemical staining of Mannosidase II (red) in HEK293 cells for identification of the Golgi zone and comparison to the expression pattern obtained with the hQC−EGFP fusion protein (green) in HEK293. An overlay of hQC and Mannosidase II suggests colocalization within the Golgi zone (merge). (B) Expression of hQC−EGFP protein (green) and APP(NLE) (red) in HEK293 cells. An overlay of hQC and APP(NLE) suggests a colocalization at least within the Golgi compartment (merge).

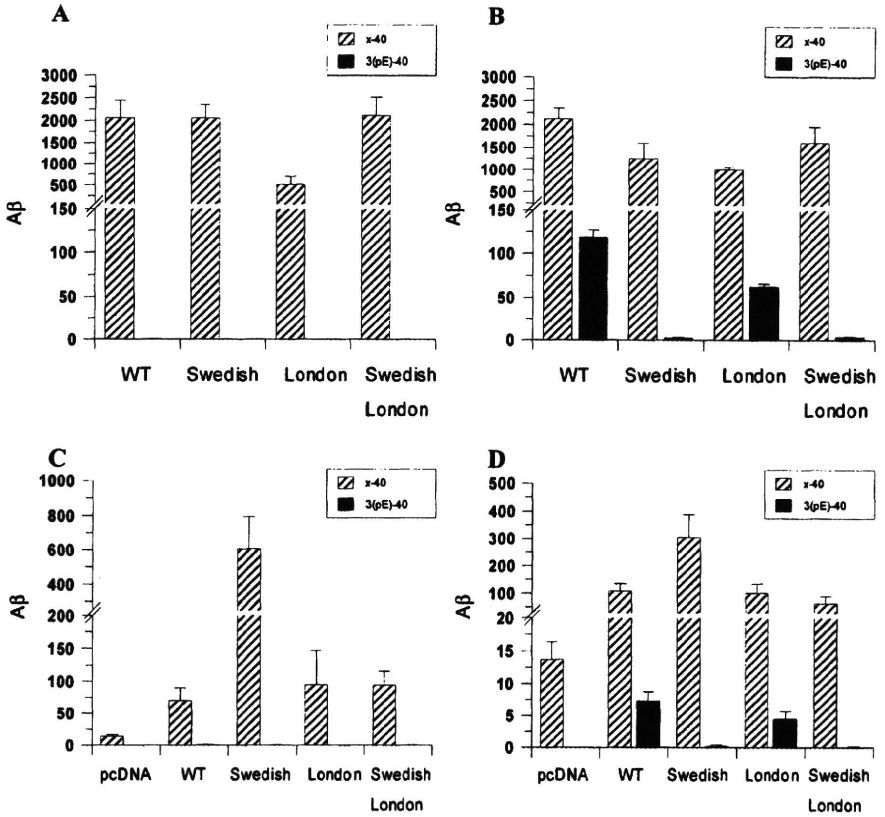

FIGURE 5: N-Terminal variants generated by the expression of FAD mutants and APP(WT) in HEK293 cells (A and B) and LNZ308 cells (C and D). The formation of $A\beta_{3(pE)-40}$ was investigated in the absence (A and C) and presence (B and D) of an E599Q (N3Q) mutation. The $A\beta$ concentration was determined using ELISAs specific for $A\beta_{x-40}$ and $A\beta_{3(pE)-40}$ and normalized to cell count (picograms per milliliter per 1×10^6 cells).

formation of $A\beta_{3(pE)-42}$. Furthermore, the addition of recombinant human QC to the cell culture medium of APP(NLE)-expressing cells generated only minor amounts of $A\beta_{3(pE)-42}$ compared to the human QC cotransfection (Figure 3). The determination of QC activity after incubation for 24 h on the cells showed a 2-fold higher activity, when recombinant QC was applied, in comparison to the coexpression of APP(NLE) and human QC. This result supports the assumption that cyclization of glutamate is favored in intracellular compartments. This was further substantiated by an immunohistochemical analysis of the subcellular distribution of human QC and APP(NLE) in HEK293 cells. A cDNA construct was generated encoding human QC, which was fused to the enhanced green fluorescent protein (EGFP). The expression of the QC−EGFP fusion protein led to a vesicular staining within the expressing cells. HEK293 cells were counterstained using an anti-Mannosidase II antibody as a marker protein for the Golgi complex. Superimpositions of the resulting images show that human QC colocalizes within the Golgi complex with Mannosidase II, substantiating the localization of QC in the secretory compartments (Figure 4A). Coexpression of human QC−EGFP fusion protein with APP(NLE) clearly supports partial colocalzation in the secretory pathway, as revealed by a counterstaining with anti-β-amyloid antibody 6E10 (Figure 4B).

Formation of N-Truncated Aβ Peptides Is Influenced by the β-Secretase Cleavage Site. The removal of the dipeptide Asp-Ala from the N-terminus of $A\beta_{1(D)-x}$ must precede the formation of $A\beta_{3(pE)}$ in vivo. It remains unclear whether the pGlu precursor $A\beta_{3(E)}$ is sequentially liberated by β-secretase and an aminopeptidase or is generated directly by endoproteolysis of APP by a yet unknown mechanism. The impact of FAD mutations on the N-terminal composition of $A\beta$ peptides was investigated using ELISAs, which discriminate between intact N-terminal $A\beta_{1(D)-40/42}$ or N-truncated $A\beta_{x-40/42}$ peptides. Introduction of the KM595/596NL Swedish mutation into the APP695 sequence led preferentially to the generation of $A\beta$ molecules possessing an intact N-terminus. However, the K595/M596 WT sequence at the β-secretase cleavage site produced prominent amounts of $A\beta$ peptides differing from $A\beta_{1(D)}$ at the N-terminus. Only 21% of $A\beta_{x-40}$ corresponded to $A\beta_{1(D)-40}$ and 46% of $A\beta_{x-42}$ to $A\beta_{1(D)-42}$, if APP(WT) was expressed. In contrast, the Swedish mutation within the APP sequence provoked generation of $A\beta$ peptides with an intact N-terminus (not shown).

To investigate the influence of the β-cleavage on $A\beta_{3(pE)-42}$ formation, we introduced a novel E599Q (N3Q) point mutation into APP(WT), APP(Swedish), APP(London), and APP(Swedish/London), allowing the sensitive and specific detection of $A\beta$ species, which are N-terminally truncated. Upon N-terminal cleavage, glutamine is readily cyclized to pGlu as observed with the APP(NLQ) construct (Figure 2A,B). Thus, the N3Q mutation within the applied FAD-APP mutants and APP(WT) serves as a monitoring mutation for the generation of N-truncated $A\beta$ peptides starting with a pGlu residue in position 3. All APP variants were expressed in the absence (Figure 5A,C) and presence (Figure 5B,D) of the N3Q mutation in HEK293 cells (Figure 5A,B) and

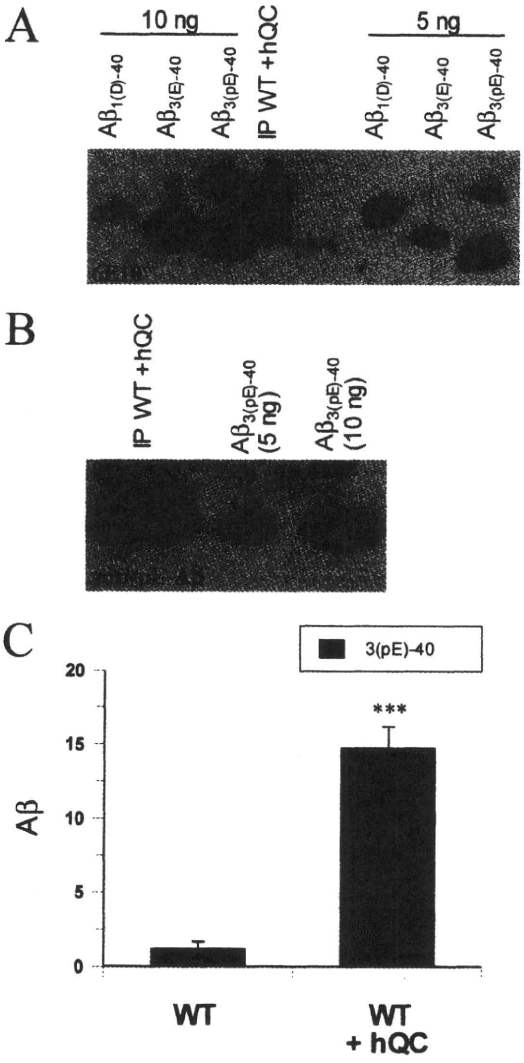

FIGURE 6: QC-dependent pGlu formation of APP(WT) was investigated by Western blotting after immunoprecipitation of Aβ peptides (application in comparison to standard Aβ peptides) using antibody 6E10, detecting total-Aβ (A) and antibody detecting pGlu-modified Aβ (B). (C) QC-dependent pGlu formation investigated using an ELISA after concentration of Aβ-containing cell media using centrifugal devices [single transfection of APP(WT) or cotransfection of APP(WT) with hQC] (Aβ concentration in picograms per milliliter) (asterisks, $P < 0.001$; Student's t test; $n = 5$).

LNZ308 cells (Figure 5C,D). The cell culture medium was analyzed for potential $A\beta_{3(pE)-40}$ formation. Intriguingly, the expression of APP variants containing the N3Q mutation led only in the case of APP(WT) and APP(London) to significant amounts of $A\beta_{3(pE)-40}$, whereas the presence of the Swedish mutation resulted only in scarce amounts of $A\beta_{3(pE)-40}$. This result was also observed when $A\beta_{3(pE)-42}$ was analyzed, pointing to differences in the liberation of Aβ peptides from APP molecules bearing the APP(WT) and APP(Swedish) sequence at the β-secretase cleavage site.

These significant differences in the liberation of N-truncated Aβ peptides prompted us to investigate the formation of $A\beta_{3(pE)}$ from APP(WT). As described for the APP(NLE) construct, cotransfection of APP(WT) and human QC was implemented to facilitate the formation of $A\beta_{3(pE)}$. On the basis of the urea−PAGE Western blot analysis, two different Aβ forms were detected (Figure 6A). The lower band corresponds to $A\beta_{3(pE)-40}$, whereas the upper band migrates slower than $A\beta_{1(D)-40}$, again suggesting an N-terminus differing from that of full-length Aβ, observed for APP(WT) expression. In addition, the results obtained by IP−Western blot analysis were validated by application of a pGlu-specific antibody (Figure 6B) and by concentration of the supernatant in centrifugal devices, followed by an ELISA, revealing significant $A\beta_{3(pE)-40}$ formation after cotransfection of APP(WT) and human QC (Figure 6C).

DISCUSSION

The Aβ peptides of amyloid deposits in brains of patients with Alzheimer's disease display a profound N- and C-terminal heterogeneity (*7, 11, 29*). Cleavage of γ-secretase causes primarily the C-terminal differences. Because neuritic plaques are mainly composed of $A\beta_{42}$, and the deposition of $A\beta_{42}$ precedes that of $A\beta_{40}$, $A\beta_{42}$ is thought to be more amyloidogenic than $A\beta_{40}$ (*27, 30*). The role and formation of N-terminal modifications, however, are more poorly understood. In particular, it is known that truncated Aβ peptides possessing a pGlu residue at the N-terminus are highly abundant in affected brains of patients with Alzheimer's disease and Down syndrome (*11, 12, 14*). Furthermore, the amyloidogenic peptides ABri in familial British dementia (FBD) and ADan in familial Danish dementia (FDD) possess an N-terminal pGlu residue, and pGlu formation appears to be crucial for the deposition of the ADan peptides in vivo (*31, 32*). Moreover, these pGlu-modified peptides have been shown to seed the aggregation of $A\beta_{1(D)-42}$ (*17*). Therefore, the prevention of pGlu formation might represent a new concept for the causal treatment of Alzheimer's disease and other pGlu-related amyloidoses.

However, the generation of pGlu peptides in AD, FBD, and FDD remained elusive, leaving room for speculation about their generation. In addition, despite evidence of an early role of pGlu-Aβ in the development of Alzheimer's disease, the formation of pGlu-Aβ peptides is frequently considered as a spontaneous secondary reaction occurring late in the progression of the disease (*33*). It should be noted that the uncatalyzed cyclization of N-terminal glutamic acid occurs exceptionally slowly, with half-lifes of years to decades under in vivo conditions (*43, 44*). In addition, since Aβ anabolism and catabolism make up a homeostasis showing a high rate of daily turnover, it is conceivable to assume an enzyme-catalyzed formation of pGlu-Aβ peptides. On the basis of artificial peptide substrates, recent in vitro studies provided the first evidence that glutamate cyclization at the N-terminus of Aβ might be due to catalysis of QC (*21, 22*). These results are highlighted here by the proof that the formation of $A\beta_{3(pE)-40/42}$ from glutamate occurs after amyloidogenic processing of APP. Most importantly, we describe for the first time the generation of $A\beta_{3(pE)}$ after expression of APP(WT), which is present in the vast majority of all AD cases, substantiating the assumption that QC might be a novel drug target for the treatment of pGlu-related amyloidoses.

According to the previous investigations of substrate specificity, the QC-catalyzed cyclization of glutamate requires a protonated γ-carboxyl group and an unprotonated α-amino group. The highest concentrations of these species are found under mildly acidic conditions around pH 6.0 (*21*). Similar pH conditions have been described for the secretory compartments

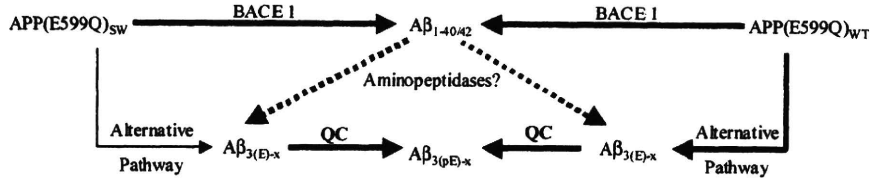

FIGURE 7: Proposed mechanism for the generation of N-terminally truncated Aβ peptides. Aβ is naturally liberated by N-terminal proteolysis due to BACE I, leading to $Aβ_{1(D)-40/42}$. This full-length Aβ species can be truncated by aminopeptidases. However, significant differences were observed for the generation of $Aβ_{3(pE)-x}$ between $APP(E599Q)_{WT}$ and $APP(E599Q)_{SW}$. Obviously, an alternative pathway exists, which is more pronounced for the $APP(E599Q)_{WT}$ variant. This leads to the generation of N-truncated $Aβ_{3(E)-x}$ species, which can be further cyclized by QC to obtain $Aβ_{3(pE)-x}$. Whether the alternative pathway represents different subcellular sites of BACE I-mediated Aβ liberation or a BACE I-independent mechanism has to be further addressed.

(*37*). As summarized in Figure 4, APP and QC are colocalized at least within the Golgi complex, where a spatially high concentration of both QC and Aβ or the respective β-CTFs can be expected (*34–36*). In this regard, these data suggest that the colocalization of QC and Aβ enhances pGlu-Aβ formation (Figure 3) and further support a catalyzed generation of this peptide species. In addition, the accumulation of pGlu-Aβ might also contribute to the intracellular aggregation of Aβ, which is frequently detected in patients with Down syndrome and Alzheimer's disease (*38–41*), in terms of generating the initial insoluble seeds for further Aβ deposition. The seeding capability of pGlu-Aβ was recently investigated in vitro, supporting the possibility that pGlu-Aβ can initiate seeding of full-length Aβ peptides (*17*).

Although these results strongly imply a QC-catalyzed formation of $Aβ_{3(pE)}$, a molecular pathway of APP processing leading finally to the substrate $Aβ_{3(E)-x}$ has never been investigated in detail. To examine the generation of $Aβ_{3(pE)}$ from APP processing, we introduced a novel monitoring mutation [APP(E599Q)], which leads to instant pGlu formation following the release of the N-terminal amino acids of Aβ. Intriguingly, the results suggest that the WT sequence at the β-secretase cleavage results in the production of N-truncated Aβ species, whereas the Swedish mutation leads preferentially to full-length $Aβ_{1(D)-x}$ peptides (Figure 7). Apparently, the endoproteolytic processing of APP(WT) and APP(Swedish) by β-secretase differs not only in our analyzed model system. Data from studies in transgenic animals overexpressing the APP(Swedish) mutation, e.g., Tg2576, have revealed conspicuous differences with regard to the Aβ composition (*42*). AD patients display up to 50% of pGlu-Aβ deposited as an early Aβ species. These mouse models, in stark contrast, show only minor amounts of pGlu-Aβ [up to 0.5% (unpublished data)] occurring late in the life span of Tg2576 (12−15 months of age) (S. Schilling et al., manuscript in preparation). Most intriguingly, Tg2576 shows only mild, if any, cognitive deficits, whereas animal models accumulating larger amounts of pGlu-Aβ display strong cognitive decline and hippocampal neuron loss (*20*).

In conclusion, the data presented here provide for the first time evidence that (i) cyclization of glutamic acid generating $Aβ_{3(pE)-40/42}$ is facilitated by QC after amyloidogenic processing of APP, (ii) the localization of QC and APP and the significant formation of $Aβ_{3(pE)-40/42}$ after coexpression point to a primarily intracellular pGlu generation, and (iii) the generation of N-truncated Aβ, accounting for the majority of Aβ in AD and DS, is possibly mediated by an alternative pathway of APP processing. The latter result is reflected in the unexpected finding of tremendous $Aβ_{3(pE)-40/42}$ formation in an APP(E599Q) variant, suggesting that the WT sequence at the β-cleavage site leads to Aβ molecules that are prone to cyclization by QC (Figure 7).

The results thus strongly imply that the majority of the pGlu peptides deposited in AD and DS brains are formed by enzymatic catalysis following processing of APP(WT). QC activity, mediated by the neurotoxic potential of $Aβ_{3(pE)-40/42}$, might be involved in the first intracellular events of the amyloid cascade, potentially driving the aggregation process of Aβ. The enhanced aggregation propensity and stability of pyroglutamated Aβ, in turn, might trigger the aggregation of other Aβ species, which are generated by β- and γ-secretase at higher levels. Accordingly, the prevention of pGlu-Aβ formation might represent a novel concept for a causal treatment of Alzheimer's disease.

ACKNOWLEDGMENT

We thank Dr. Torsten Hoffmann for helpful discussion and Anett Stephan for technical assistance. We also thank Dr. Steffen Rossner (Paul-Flechsig Institut for Brain Research, Leipzig, Germany) for the access to the laser-scanning microscope. The help of Jan Eggert in critically reading the manuscript is also gratefully acknowledged.

REFERENCES

1. Saido, T. C., and Iwata, N. (2006) Metabolism of amyloid β peptide and pathogenesis of Alzheimer's disease. Towards presymptomatic diagnosis, prevention and therapy. *Neurosci. Res. 54*, 235–253.
2. Selkoe, D. J. (2001) Alzheimer's disease: Genes, proteins, and therapy. *Physiol. Rev. 81*, 741–766.
3. Esler, W. P., and Wolfe, M. S. (2001) A portrait of Alzheimer secretases: New features and familiar faces. *Science 293*, 1449–1454.
4. Haass, C., Schlossmacher, M. G., Hung, A. Y., Vigo-Pelfrey, C., Mellon, A., Ostaszewski, B. L., Lieberburg, I., Koo, E. H., Schenk, D., Teplow, D. B., and Selkoe, D. J. (1992) Amyloid β-peptide is produced by cultured cells during normal metabolism. *Nature 359*, 322–325.
5. El Mouedden, M., Vandermeeren, M., Meert, T., and Mercken, M. (2006) Reduction of Aβ levels in the Sprague Dawley rat after oral administration of the functional γ-secretase inhibitor, DAPT: A novel non-transgenic model for Aβ production inhibitors. *Curr. Pharm. Des. 12*, 671–676.
6. Saido, T. C. (1998) Alzheimer's disease as proteolytic disorders: Anabolism and catabolism of β-amyloid. *Neurobiol. Aging 19*, S69−S75.
7. Saido, T. C., Yamao-Harigaya, W., Iwatsubo, T., and Kawashima, S. (1996) Amino- and carboxyl-terminal heterogeneity of β-amyloid peptides deposited in human brain. *Neurosci. Lett. 215*, 173–176.
8. Sergeant, N., Bombois, S., Ghestem, A., Drobecq, H., Kostanjevecki, V., Missiaen, C., Wattez, A., David, J. P., Vanmechelen, E., Sergheraert, C., and Delacourte, A. (2003) Truncated β-amyloid peptide species in pre-clinical Alzheimer's disease as new targets for the vaccination approach. *J. Neurochem. 85*, 1581–1591.
9. Jarrett, J. T., Berger, E. P., and Lansbury, P. T., Jr. (1993) The carboxy terminus of the β amyloid protein is critical for the seeding

of amyloid formation: Implications for the pathogenesis of Alzheimer's disease. *Biochemistry 32*, 4693–4697.
10. Roher, A. E., Palmer, K. C., Yurewicz, E. C., Ball, M. J., and Greenberg, B. D. (1993) Morphological and biochemical analyses of amyloid plaque core proteins purified from Alzheimer disease brain tissue. *J. Neurochem. 61*, 1916–1926.
11. Saido, T. C., Iwatsubo, T., Mann, D. M., Shimada, H., Ihara, Y., and Kawashima, S. (1995) Dominant and differential deposition of distinct β-amyloid peptide species, Aβ N3(pE), in senile plaques. *Neuron 14*, 457–466.
12. Russo, C., Saido, T. C., DeBusk, L. M., Tabaton, M., Gambetti, P., and Teller, J. K. (1997) Heterogeneity of water-soluble amyloid β-peptide in Alzheimer's disease and Down's syndrome brains. *FEBS Lett. 409*, 411–416.
13. Russo, C., Salis, S., Dolcini, V., Venezia, V., Song, X. H., Teller, J. K., and Schettini, G. (2001) Amino-terminal modification and tyrosine phosphorylation of carboxy-terminal fragments of the amyloid precursor protein in Alzheimer's disease and Down's syndrome brain. *Neurobiol. Dis. 8*, 173–180.
14. Hosoda, R., Saido, T. C., Otvos, L., Arai, T., Mann, D. M., Lee, V. M., Trojanowski, J. Q., and Iwatsubo, T. (1998) Quantification of modified amyloid β peptides in Alzheimer disease and Down syndrome brains. *J. Neuropathol. Exp. Neurol. 57*, 1089–1095.
15. Harigaya, Y., Saido, T. C., Eckman, C. B., Prada, C. M., Shoji, M., and Younkin, S. G. (2000) Amyloid β protein starting pyroglutamate at position 3 is a major component of the amyloid deposits in the Alzheimer's disease brain. *Biochem. Biophys. Res. Commun. 276*, 422–427.
16. Russo, C., Violani, E., Salis, S., Venezia, V., Dolcini, V., Damonte, G., Benatti, U., D'Arrigo, C., Patrone, E., Carlo, P., and Schettini, G. (2002) Pyroglutamate-modified amyloid β-peptides—AβN3(pE)—strongly affect cultured neuron and astrocyte survival. *J. Neurochem. 82*, 1480–1489.
17. Schilling, S., Lauber, T., Schaupp, M., Manhart, S., Scheel, E., Bohm, G., and Demuth, H. U. (2006) On the seeding and oligomerization of pGlu-amyloid peptides (in vitro). *Biochemistry 45*, 12393–12399.
18. He, W., and Barrow, C. J. (1999) The Aβ 3-pyroglutamyl and 11-pyroglutamyl peptides found in senile plaque have greater β-sheet forming and aggregation propensities in vitro than full-length Aβ. *Biochemistry 38*, 10871–10877.
19. Piccini, A., Russo, C., Gliozzi, A., Relini, A., Vitali, A., Borghi, R., Giliberto, L., Armirotti, A., D'Arrigo, C., Bachi, A., Cattaneo, A., Canale, C., Torrassa, S., Saido, T. C., Markesbery, W., Gambetti, P., and Tabaton, M. (2005) β-Amyloid is different in normal aging and in Alzheimer's disease. *J. Biol. Chem. 280*, 34186–34192.
20. Casas, C., Sergeant, N., Itier, J. M., Blanchard, V., Wirths, O., van der, K. N., Vingtdeux, V., van de, S. E., Ret, G., Canton, T., Drobecq, H., Clark, A., Bonici, B., Delacourte, A., Benavides, J., Schmitz, C., Tremp, G., Bayer, T. A., Benoit, P., and Pradier, L. (2004) Massive CA1/2 neuronal loss with intraneuronal and N-terminal truncated Aβ42 accumulation in a novel Alzheimer transgenic model. *Am. J. Pathol. 165*, 1289–1300.
21. Schilling, S., Hoffmann, T., Manhart, S., Hoffmann, M., and Demuth, H. U. (2004) Glutaminyl cyclases unfold glutamyl cyclase activity under mild acid conditions. *FEBS Lett. 563*, 191–196.
22. Cynis, H., Schilling, S., Bodnar, M., Hoffmann, T., Heiser, U., Saido, T. C., and Demuth, H. U. (2006) Inhibition of glutaminyl cyclase alters pyroglutamate formation in mammalian cells. *Biochim. Biophys. Acta 1764*, 1618–1625.
23. Shirotani, K., Tsubuki, S., Lee, H. J., Maruyama, K., and Saido, T. C. (2002) Generation of amyloid β peptide with pyroglutamate at position 3 in primary cortical neurons. *Neurosci. Lett. 327*, 25–28.
24. Klafki, H. W., Wiltfang, J., and Staufenbiel, M. (1996) Electrophoretic separation of βA4 peptides (1−40) and (1−42). *Anal. Biochem. 237*, 24–29.
25. Schilling, S., Hoffmann, T., Wermann, M., Heiser, U., Wasternack, C., and Demuth, H. U. (2002) Continuous spectrometric assays for glutaminyl cyclase activity. *Anal. Biochem. 303*, 49–56.
26. Citron, M., Oltersdorf, T., Haass, C., McConlogue, L., Hung, A. Y., Seubert, P., Vigo-Pelfrey, C., Lieberburg, I., and Selkoe, D. J. (1992) Mutation of the β-amyloid precursor protein in familial Alzheimer's disease increases β-protein production. *Nature 360*, 672–674.
27. Suzuki, N., Cheung, T. T., Cai, X. D., Odaka, A., Otvos, L., Jr., Eckman, C., Golde, T. E., and Younkin, S. G. (1994) An increased percentage of long amyloid β protein secreted by familial amyloid β protein precursor (βAPP717) mutants. *Science 264*, 1336–1340.
28. Schilling, S., Hoffmann, T., Rosche, F., Manhart, S., Wasternack, C., and Demuth, H. U. (2002) Heterologous expression and characterization of human glutaminyl cyclase: Evidence for a disulfide bond with importance for catalytic activity. *Biochemistry 41*, 10849–10857.
29. Kuo, Y. M., Emmerling, M. R., Woods, A. S., Cotter, R. J., and Roher, A. E. (1997) Isolation, chemical characterization, and quantitation of Aβ 3-pyroglutamyl peptide from neuritic plaques and vascular amyloid deposits. *Biochem. Biophys. Res. Commun. 237*, 188–191.
30. Iwatsubo, T., Odaka, A., Suzuki, N., Mizusawa, H., Nukina, N., and Ihara, Y. (1994) Visualization of Aβ42(43) and Aβ40 in senile plaques with end-specific Aβ monoclonals: Evidence that an initially deposited species is Aβ42(43). *Neuron 13*, 45–53.
31. Tomidokoro, Y., Lashley, T., Rostagno, A., Neubert, T. A., Bojsen-Moller, M., Braendgaard, H., Plant, G., Holton, J., Frangione, B., Revesz, T., and Ghiso, J. (2005) Familial Danish dementia: Co-existence of Danish and Alzheimer amyloid subunits (ADan AND Aβ) in the absence of compact plaques. *J. Biol. Chem. 280*, 36883–36894.
32. Ghiso, J., Revesz, T., Holton, J., Rostagno, A., Lashley, T., Houlden, H., Gibb, G., Anderton, B., Bek, T., Bojsen-Moller, M., Wood, N., Vidal, R., Braendgaard, H., Plant, G., and Frangione, B. (2001) Chromosome 13 dementia syndromes as models of neurodegeneration. *Amyloid 8*, 277–284.
33. Hashimoto, T., Wakabayashi, T., Watanabe, A., Kowa, H., Hosoda, R., Nakamura, A., Kanazawa, I., Arai, T., Takio, K., Mann, D. M., and Iwatsubo, T. (2002) CLAC: A novel Alzheimer amyloid plaque component derived from a transmembrane precursor, CLAC-P/collagen type XXV. *EMBO J. 21*, 1524–1534.
34. Greenfield, J. P., Tsai, J., Gouras, G. K., Hai, B., Thinakaran, G., Checler, F., Sisodia, S. S., Greengard, P., and Xu, H. (1999) Endoplasmic reticulum and trans-Golgi network generate distinct populations of Alzheimer β-amyloid peptides. *Proc. Natl. Acad. Sci. U.S.A. 96*, 742–747.
35. Hartmann, T., Bieger, S. C., Bruhl, B., Tienari, P. J., Ida, N., Allsop, D., Roberts, G. W., Masters, C. L., Dotti, C. G., Unsicker, K., and Beyreuther, K. (1997) Distinct sites of intracellular production for Alzheimer's disease Aβ40/42 amyloid peptides. *Nat. Med. 3*, 1016–1020.
36. Fischer, W. H., and Spiess, J. (1987) Identification of a mammalian glutaminyl cyclase converting glutaminyl into pyroglutamyl peptides. *Proc. Natl. Acad. Sci. U.S.A. 84*, 3628–3632.
37. Demaurex, N., Furuya, W., D'Souza, S., Bonifacino, J. S., and Grinstein, S. (1998) Mechanism of acidification of the trans-Golgi network (TGN). In situ measurements of pH using retrieval of TGN38 and furin from the cell surface. *J. Biol. Chem. 273*, 2044–2051.
38. Gouras, G. K., Almeida, C. G., and Takahashi, R. H. (2005) Intraneuronal Aβ accumulation and origin of plaques in Alzheimer's disease. *Neurobiol. Aging 26*, 1235–1244.
39. Mori, C., Spooner, E. T., Wisniewsk, K. E., Wisniewski, T. M., Yamaguch, H., Saido, T. C., Tolan, D. R., Selkoe, D. J., and Lemere, C. A. (2002) Intraneuronal Aβ42 accumulation in Down syndrome brain. *Amyloid 9*, 88–102.
40. Gouras, G. K., Tsai, J., Naslund, J., Vincent, B., Edgar, M., Checler, F., Greenfield, J. P., Haroutunian, V., Buxbaum, J. D., Xu, H., Greengard, P., and Relkin, N. R. (2000) Intraneuronal Aβ42 accumulation in human brain. *Am. J. Pathol. 156*, 15–20.
41. Gyure, K. A., Durham, R., Stewart, W. F., Smialek, J. E., and Troncoso, J. C. (2001) Intraneuronal Aβ-amyloid precedes development of amyloid plaques in Down syndrome. *Arch. Pathol. Lab. Med. 125*, 489–492.
42. Kawarabayashi, T., Younkin, L. H., Saido, T. C., Shoji, M., Ashe, K. H., and Younkin, S. G. (2001) Age-dependent changes in brain, CSF, and plasma amyloid β protein in the Tg2576 transgenic mouse model of Alzheimer's disease. *J. Neurosci. 21*, 372–381.
43. Yu, L., Vizel, A., Huff, M. B., Young, M., Remmele, R. L., Jr., and He, B. (2006) Investigation of N-terminal glutamate cyclization of recombinant monoclonal antibody in formulation development. *J. Pharm. Biomed. Anal. 42*, 455–463.
44. Chelius, D., Jing, K., Lueras, A., Rehder, D. S., Dillon, T. M., Vizel, A., Rajan, R. S., Li, T., Treuheit, M. J., and Bondarenko, P. V. (2006) Formation of pyroglutamic acid from N-terminal glutamic acid in immunoglobulin γ antibodies. *Anal. Chem. 78*, 2370–2376.

BI800250P

BMC Cardiovascular Disorders

BioMed Central

Research article

Open Access

Activation of calpain-1 in human carotid artery atherosclerotic lesions

Isabel Gonçalves[1,2], Mihaela Nitulescu[1], Takaomi C Saido[3], Nuno Dias[4], Luis M Pedro[5], José Fernandes e Fernandes[5], Mikko PS Ares[1] and Isabella Pörn-Ares*[6,7]

Address: [1]Department of Clinical Sciences, Lund University, Malmö, Sweden, [2]Department of Cardiology and Internal Medicine, Lund University, Malmö, Sweden, [3]Laboratory for Proteolytic Neuroscience, RIKEN Brain Science Institute, 2-1 Hirosawa, Wako-shi Saitama 351-0198, Japan, [4]Department of Vascular Diseases Malmö-Lund, Lund University, Malmö, Sweden, [5]Instituto Cardiovascular de Lisboa, Lisbon, Portugal, [6]Department of Laboratory Medicine/Experimental Pathology, Lund University, Malmö, Sweden and [7]Research Program of Molecular Neurology, Institute of Biomedicine/Biochemistry, University of Helsinki, Helsinki, Finland

Email: Isabel Gonçalves - isabel.goncalves@med.lu.se; Mihaela Nitulescu - mihaela.nitulescu@med.lu.se; Takaomi C Saido - saido@brain.riken.jp; Nuno Dias - nuno.dias@med.lu.se; Luis M Pedro - lmendespedro@clix.pt; José Fernandes e Fernandes - jffernandes@netcabo.pt; Mikko PS Ares - mikko.ares@pp.inet.fi; Isabella Pörn-Ares* - isabella.ares@helsinki.fi

* Corresponding author

Published: 18 June 2009

BMC Cardiovascular Disorders 2009, **9**:26 doi:10.1186/1471-2261-9-26

Received: 9 December 2008
Accepted: 18 June 2009

This article is available from: http://www.biomedcentral.com/1471-2261/9/26

Abstract

Background: In a previous study, we observed that oxidized low-density lipoprotein-induced death of endothelial cells was calpain-1-dependent. The purpose of the present paper was to study the possible activation of calpain in human carotid plaques, and to compare calpain activity in the plaques from symptomatic patients with those obtained from patients without symptoms.

Methods: Human atherosclerotic carotid plaques (n = 29, 12 associated with symptoms) were removed by endarterectomy. Calpain activity and apoptosis were detected by performing immunohistochemical analysis and TUNEL assay on human carotid plaque sections. An antibody specific for calpain-proteolyzed α-fodrin was used on western blots.

Results: We found that calpain was activated in all the plaques and calpain activity colocalized with apoptotic cell death. Our observation of autoproteolytic cleavage of the 80 kDa subunit of calpain-1 provided further evidence for enzyme activity in the plaque samples. When calpain activity was quantified, we found that plaques from symptomatic patients displayed significantly lower calpain activity compared with asymptomatic plaques.

Conclusion: These novel results suggest that calpain-1 is commonly active in carotid artery atherosclerotic plaques, and that calpain activity is colocalized with cell death and inversely associated with symptoms.

Background

Calpains are calcium-dependent cysteine proteases that are known to be involved in the proteolysis of a number of proteins during mitosis and cell death [1,2]. The calpains constitute a large family of distinct isozymes that differ in structure and distribution [3], and three members of this family are ubiquitous – calpain-1 (μ-calpain), calpain-2 (m-calpain), and calpain-10. A study with embry-

onic fibroblasts from mice with genetically disrupted *capn4*, which codes for the regulatory subunit of both calpain-1 and -2, showed that calpains are required for activation of caspase-12 and c-Jun N-terminal kinase in ER-stress-induced apoptosis [4]. The specific endogenous protein inhibitor calpastatin, which modulates calpain activity *in vivo*, is cleaved during apoptosis [5]. The cytoskeletal protein α-fodrin is another death substrate that may be cleaved by calpains or caspases [1,6]. Additional calpain substrates known to be involved in apoptosis are Bax [7], Bid [8], p53 [9], and procaspase-3, -7, -8, and -9 [10,11]. In a previous study, we found that oxidized low-density lipoprotein (oxLDL)-induced death of human microvascular endothelial cells (HMEC-1) was accompanied by activation of calpain-1 [12]. The calpain-1 inhibitor, PD 151746, decreased oxLDL-induced cytotoxicity, and the 80 kDa subunit of calpain-1 was autoproteolytically cleaved in oxLDL-treated HMEC-1 cells, indicating that the enzyme was activated. The Bcl-2 protein Bid was also cleaved during oxLDL-elicited cell death, and this was prevented by calpain inhibitors, but not by inhibitors of cathepsin B or caspases.

Vascular calcification is present in 80% of significant atherosclerotic lesions and in at least 90% of patients with coronary artery disease [13]. Calcification can apparently begin at any point of plaque formation and seems to be a complex mechanism [14]. Since vascular calcification has been shown to correlate with elevated serum calcium [15], and oxLDL plays a central role in atherogenesis [16], we hypothesized that calpains may be activated in atherosclerotic lesions. Therefore, the primary aim of the present study was to analyze atherosclerotic plaques for possible calpain activity.

Methods

Materials

Anti-calpain-1 large subunit monoclonal Ab was from Chemicon International (Temecula, CA, MAB3082), anti-α-tubulin monoclonal Ab was from Oncogene Research Products (Boston, MA, #CP06). HRP-coupled goat anti-rabbit and goat anti-mouse immunoglobulins were from Dako A/S (Glostrup, Denmark). Reagents not listed here were obtained from Sigma, unless otherwise stated in the text.

Atherosclerotic plaques

Twenty-nine human atherosclerotic carotid plaques, from 26 patients (67 ± 8 years old, 21 males), were removed *en bloc* by carotid endarterectomy by one surgeon. Twelve plaques were associated with ipsilateral hemispheric symptoms in the last month and 17 were not associated to any symptoms after neurologic evaluation. Cardiovascular risk factors such as hypertension (systolic blood pressure > 140 mmHg), diabetes, coronary artery disease, tobacco use (in the past or current) and dyslipidemia were recorded, as well as the medication of these patients. Patients with atrial fibrillation, aortic valve disease, mechanic heart valves, ipsilateral carotid artery occlusion or restenosis after previous carotid endarterectomy were excluded. Informed consent was given by each patient. The study was approved by the local ethical committee. The histological characteristics of symptomatic and asymptomatic plaque samples have been published previously [17]. In short, carotid plaques from symptomatic patients have shown lower levels of hydroxyapatite, higher levels of elastin, cholesterol esters, unesterified cholesterol, triglycerides, more cells, DNA, and soluble protein [18] compared to those from asymptomatic patients.

Sample Preparation

The plaques removed by endarterectomy were cleaned with isotonic NaCl containing heparin (5 U/ml), to avoid blood contamination, and thereafter the plaques were immediately snap frozen in liquid nitrogen. Two-mm-thick fragments from the stenotic region of the frozen plaques were removed for histology. Plaques were weighed, cut into pieces while still frozen, and homogenized as previously described [19]. An aliquot was taken from each plaque for western blot analysis, and protein content was analyzed by the method of Lowry.

Immunoblotting and calpain activity

Loading buffer (final concentrations: 50 mmol/L Tris-HCl [pH 6,8], 2% SDS, 10% glycerol, 0,1% bromophenol blue, and 30 mmol/L dithiothreitol) was added to homogenized samples, and they were heated to 90°C in a heating block for 5 min. Proteins were separated under reducing conditions in SDS-polyacrylamide gels and then Western blotted onto PVDF filters. Blots were blocked with Tris-buffered saline containing 5% dry milk powder, and then incubated for 1–2 h with anti-proteolyzed 150 kDa α-fodrin pAb [20](diluted 1:200), anti-α-tubulin mAb (1:500), or anti-calpain-1 mAb (1:2000). The blots were subsequently incubated with a peroxidase-conjugated secondary Ab, and bound Ab was assayed by enhanced chemiluminescence detection (Santa Cruz Biotechnology, Santa Cruz, CA). To estimate the level of calpain activity, we performed densitometric analysis of Western blots with a Fluor-S MultiImager (Bio-Rad, Rockford, IL). The optical density of 150 kDa α-fodrin bands and tubulin bands was scanned, and the calculated ratio ($OD_{\alpha\text{-fodrin}}/OD_{\text{tubulin}}$) for each plaque sample was used in statistical analysis.

Immunohistochemistry

Two-millimeter-thick fragments from the stenotic regions of the frozen plaques were embedded in O.C.T. compound (Tissue-Tek, Sakura), cryo-sectioned in serial 8-μm

sections, and mounted on coated slides. Tissue sections for immunohistochemistry were fixed with 4% paraformaldehyde in phosphate buffer. Membranes were permeabilized in 0.5% Triton X-100. Endogenous peroxidase activity was quenched by incubating sections for 5 min in 0.9% H_2O_2. Thereafter sections were blocked with 10% goat serum in PBS for 30 min. Primary antibody, rabbit anti-cleaved-α-fodrin (150 kDa; ref. [20]), was diluted 1:200 and incubated overnight at 4°C in a humidified chamber. Sections were incubated with biotinylated secondary Ab (goat anti-rabbit, Vector Laboratories, Burlingame, CA) at a dilution of 1:200 for 60 min. Thereafter, sections were incubated with peroxidase- or alkaline phosphatase-labeled Streptavidin (for brown or blue stain, respectively; Vectastain ABC-AP kit, Vector Laboratories). In the case of double-staining, TUNEL was performed after the anti-cleaved-α-fodrin staining. Sections were developed with diaminobenzidine (Vector Laboratories), and counterstained with hematoxylin. Negative controls included substitution of the primary Ab with phosphate buffer.

For TUNEL staining, consecutive tissue sections were fixed with 4% paraformaldehyde in phosphate buffer and stained for apoptosis, using TUNEL *In Situ* Cell Death detection kit POD (Roche Applied Science, Indianapolis, USA), according to the manufacturer's instructions. Samples were viewed with an Olympus BX60 microscope and photographed.

Statistical Analysis

Results were normalized to the wet weight of the plaques. We used χ^2 analyses to investigate associations with dichotomous variables. Two-group comparisons were performed with the use of the Mann-Whitney non-parametric test. Spearman's rho was used for correlation analyses. Statistical analysis was performed with the use of SPSS 12.0 for Windows.

Results

Calpain activity and apoptosis

Use of Western blot analysis and a specific antibody to detect a calpain-proteolyzed α-fodrin fragment has proven to be one of the most reliable methods to demonstrate calpain activation in cell lysates [6,20]. We employed a polyclonal antibody specific for the calpain-proteolyzed 150-kDa α-fodrin fragment [20] to determine whether calpain activation occurs in atherosclerotic plaques. We found that all plaque samples contained the calpain-generated 150-kDa α-fodrin breakdown product (Figure 1A). These results show that calpain was activated and catalysed the cleavage of α-fodrin in the atherosclerotic plaques.

The autoproteolytic cleavage of the 80 kDa subunit of calpain-1 and -2 is known to be associated with activation of these enzymes [3]. To further verify the activation of calpain in atherosclerotic plaques, we used a monoclonal antibody against the 80 kDa subunit of calpain-1 on western blots, and we observed the 78 kDa autoproteolysis product of calpain-1 in all samples (Figure 1B). The detection of cleaved calpain-1 provided further evidence for active calpain in atherosclerotic plaques.

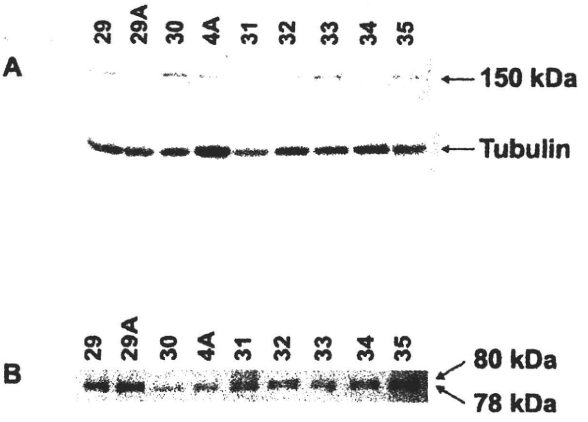

Figure 1
Calpain-1 is activated in atherosclerotic plaques and cleaves α-fodrin. A, Plaque homogenates were processed for Western blotting, and the PVDF membrane was probed with an anti-proteolyzed α-fodrin Ab specific for the 150-kDa fragment produced by calpain activity. The membrane was subsequently stripped and re-probed with anti-α-tubulin Ab as a loading control. B, same as A, except that the PVDF membrane was probed with anti-calpain-1 large subunit Ab. The blots show 9 samples (the id number of each plaque is depicted above the lanes) of 29 analyzed. All 29 samples contained the 150 kDa α-fodrin fragment as well as the autolytic fragment of calpain-1.

The preparation of homogenates for western blot analysis from plaque samples is a lengthy process, and despite the included protease inhibitors it could be argued that the proteolysis detected in Figure 1 might be artifacts from the processing of the samples. Therefore we performed immunohistochemistry on sections of the plaque samples, and the results from this analysis verified that calpain was indeed activated in the plaques. Figure 2 shows a plaque with immunohistochemical staining of the calpain-generated 150-kDa α-fodrin fragment, as well as apoptotic cell death detected by TUNEL staining. Interestingly, calpain activity (Figure 2A, B, C, and 2D) colocalized with cell death, as shown in Figure 2A, B, G, and 2H.

Calpain activity and plaque characteristics

When calpain activities were quantified from western blots, we found that symptomatic carotid plaques dis-

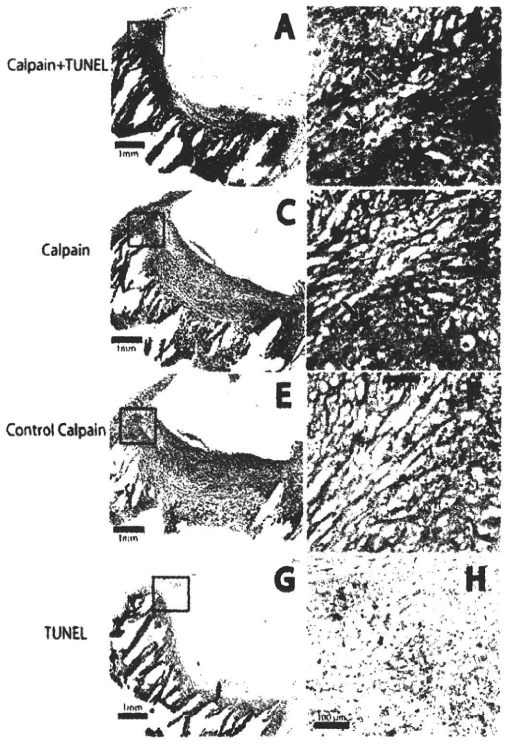

Figure 2
Immunohistochemical stainings of a human atherosclerotic plaque. The region inside the square in A, C, E, and G is amplified in B, D, F, and H, respectively. A and B, sections were double stained for calpain (proteolyzed α-fodrin, in blue) and TUNEL (in brown), showing colocalization of these two stainings. The arrows in B show cells staining positively for calpain and TUNEL. C and D, sections were incubated with anti-proteolyzed α-fodrin antibody. α-fodrin fragments, resulting from the presence of active calpain, are present in the core and shoulder regions of the plaques and in some scattered areas of the fibrous cap. This is also seen in A with the blue colour. In D, cells stained brown are positive for calpain activity (long arrow), whereas non-stained cells (short arrow) are not. E and F, negative control (primary antibody omitted). G and H, TUNEL staining for cell death (in brown). The arrow in H points to a dying cell, staining brown.

played significantly lower calpain activity (on average 38.0% less) compared with plaques not associated with symptoms (Figure 3). Since calpain-dependent apoptosis has been detected in simvastatin-treated rat vascular smooth muscle cells [21], we decided to perform statistical analyses comparing calpain activity of the plaques and statin intake. However, we found no significant difference

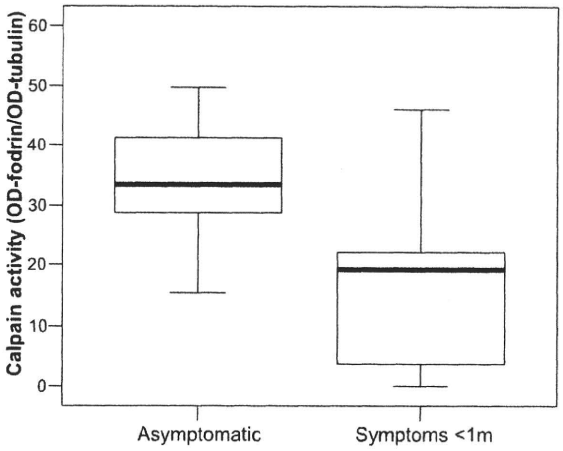

Figure 3
Differences in calpain activity of carotid plaques from asymptomatic and symptomatic patients. Calpain activity was estimated as described in Materials and Methods. The difference between asymptomatic and symptomatic plaques was statistically significant ($p = 0.034$). The box plot shows minimum, first quartile, median, third quartile, and maximum levels.

in calpain activity between untreated patients and those taking statins (data not shown). There were no significant differences in calpain activity between untreated patients and those taking anti-hypertensives (including calcium-channel blockers; Tables 1 and 2). Neither was there any significant association found between calpain activity and the registered cardiovascular risk factors.

Discussion

Our present data demonstrate unequivocally that calpain was activated in atherosclerotic plaques and that calpain activity was co-localized with cell death. Interestingly, in a previous study on these carotid plaques, those associated

Table 1: Most relevant clinical characteristics of the symptomatic patients.

Symptomatic (n = 12)	No	Yes
Diabetes	9	3
Hypertension	4	8
Heart disease	5	7
Smoking	4	current 3 and ex 5
Obesity	12	0
Family history of cardiovascular disease	11	1
Peripheral arterial disease	11	1
Statin	10	2
Anti-hypertensives	5	7 (3 CCB)

CCB, calcium channel blockers